UNIVERSITY OF CALIFORNIA, SAN DIEGO

Distributed Proxy-Layer Scheduling in Heterogeneous Wireless Sensor Networks

A thesis submitted in partial satisfaction of the requirements for the degree Master of Science

in

Computer Science

by

Daeseob Lim

Committee in charge:

Professor Tajana Simunic Rosing, Chair
Professor Geoffrey Michael Voelker
Professor Tara Javidi

2007

The Thesis of Daeseob Lim is approved:

Chair

University of California, San Diego

2007

TABLE OF CONTENTS

LIST OF FIGURES

ACKNOWLEDGEMENTS

I would first like to thank my research advisor, Tajana Simunic Rosing. Her guidance has been invaluable through all stages of this thesis. The advice from Tara Javidi and Geoffrey Michael Voelker has been greatly helpful in designing the algorithms proposed in this thesis.

I would like to thank the HPWREN project and the NSF for their support. HPWREN is based on the work sponsored by the National Science Foundation and its ANIR division under Grant Number 0426879. I also thank Hans-Werner Braun from the San Diego Supercomputer Center (SDSC) and Pablo Bryant from the San Diego State University for their help and support for the research on the HPWREN/SMER project.

I want to express my sincere gratitude to my family. I thank my mother for the sacrifices she made. My sisters always showed their faith and encouragement to me. Without their devotion, I may never have completed this thesis or even my graduate degree. Thank you for your love and support. And I thank God.

ABSTRACT OF THE THESIS

Distributed Proxy-Layer Scheduling in Heterogeneous Wireless Sensor Networks

by

Daeseob Lim

Master of Science in Computer Science

University of California, San Diego, 2007

Professor Tajana Simunic Rosing, Chair

In this thesis, we present a distributed hybrid multi-cell scheduling algorithm for heterogeneous wireless sensor networks. The proposed scheduling algorithm addresses the issues of limited power on mobile nodes and throughput degradation due to contention in multi-cell wireless networks. Our scheduling algorithm consists of two parts; cell-level scheduling and node-level scheduling.

The cell-level scheduling algorithm decides which cells are active so that the interference between active cells is reduced drastically. Node-level scheduling

algorithm decreases the contention among wireless nodes by limiting the number of active nodes accessing a wireless channel. By combining these two scheduling algorithms, we reduce energy consumption of communication devices on mobile nodes and improve aggregate throughput in multi-cell wireless networks.

The proposed scheduling algorithm is designed to run in a distributed manner. To show the efficiency of our node-level algorithm, we first give, for comparison, an optimal node-level scheduling algorithm and show that the problem is NP-complete. Finally, we present a heuristic scheduling algorithm and convert it into our distributed node-level scheduling algorithm.

We also evaluate the performance of our algorithm. Simulation results from the *ns-2* network simulator show that our scheduling is effective in saving communication power while improving throughput of multi-cell wireless networks. Our scheduling achieves a throughput improvement of up to 10.31% and maximum power saving of 85.54%.

I. INTRODUCTION

A *heterogeneous wireless network* is a wireless network system consisting of devices with various levels of computing capability, different energy constraints, and multiple types of wireless connectivity. When heterogeneous wireless networks are constructed over sensor networks, we call them *heterogeneous wireless sensor networks*. Similar to typical wireless networks, heterogeneous wireless sensor networks suffer from limited battery lifetime, excessive contention between wireless nodes, and insufficient network throughput capacity. Often heterogeneous wireless sensor network applications also have variety of quality of service (QoS) requirements.

To have wide coverage in the field and to successfully transfer heavy traffic from the sensor nodes, heterogeneous wireless sensor networks use high-bandwidth connections centered at sensor node cluster heads over the underlying sensor network. Once the traffic from the sensor nodes is collected at cluster heads, the wireless network delivers the data to a wired network backbone. Commercial wireless LAN (WLAN) such as IEEE 802.11 is a good candidate for the relay network which connects the cluster header nodes with a wired network.

An example of a heterogeneous wireless sensor network is the High-Performance Wireless Research and Education Network (HPWREN) [2] deployed in the Southern California area. As shown in Figure 1, HPWREN connects local universities, research institutes, and natural observatories through a variety of wireless and backbone networks. In HPWREN, there are many kinds of computing systems ranging from the small wireless sensor nodes, and scientists' laptops, to the high-performance server systems at the San Diego Supercomputer Center. HPWREN has several subnetworks in it. One of them is the Santa Margarita Ecological Reserve (SMER) network in Figure 2, which is a good example of a

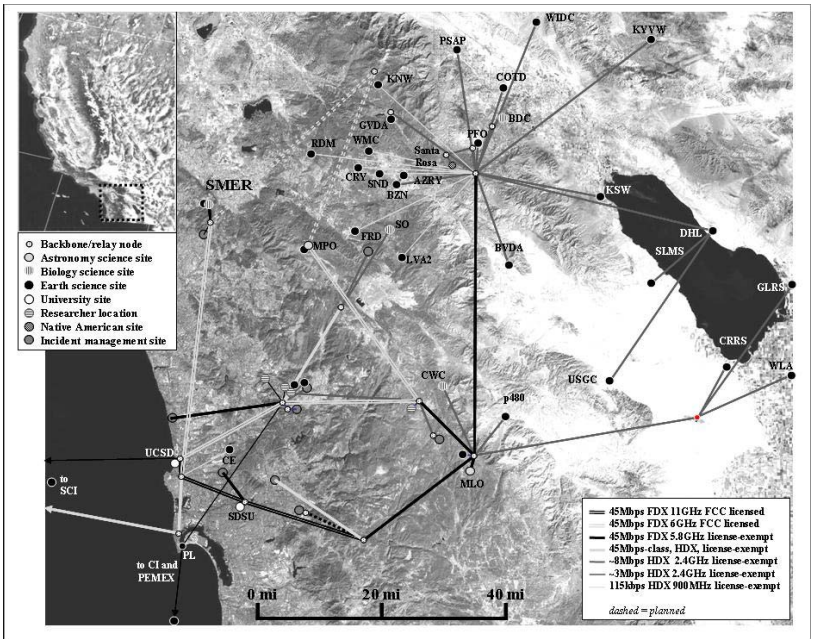

Figure 1. Network topology of HPWREN

heterogeneous wireless sensor network.

The SMER network consists of three layers of deployed wireless nodes. The lowest layer collects ecological information in the field and transfers the data to the middle layer through a typical sensor network. The middle layer is a group of child cluster heads (*child CH*s) which convey the data from sensor nodes to the parent cluster heads (*parent CH*s) through a faster wireless connection, mainly IEEE 802.11b. This middle layer is responsible for handling the heavy traffic of the underlying sensors. In this layer, the issues such as contention and interference between adjacent wireless nodes result in insufficient throughput capacity. The parent cluster heads in the upper layer connects child cluster heads to the HPWREN wireless mesh backbone.

One of the important issues in heterogeneous wireless sensor networks is the battery life of mobile wireless nodes. Typically, a large portion of the total energy in mobile devices is consumed by the wireless communication devices. In particular, the radio power

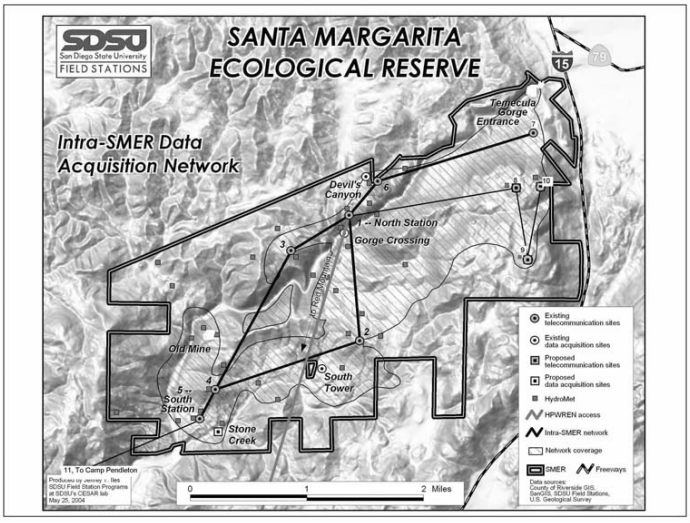

Figure 2. SMER network

consumption in an idle state of wireless devices plays a significant role in the lifetime of mobile devices. In the case of heavy congestion in a wireless channel, the issue of communication power is even more important. For example, in the middle layer of the SMER network, a parent cluster head incorporates many child cluster heads. As the child cluster heads are close to each other, their radio signals cause a high rate of interference, which results in a large number of packet collisions. Moreover, adjacent child cluster heads that join different parent cluster heads can also interfere over the same radio channel. Channel assignment may reduce the interference in the shared channels (e.g. channel interference in cellular networks). As the number of usable non-interfered channels is limited, the channel assignment cannot solve the interference problem completely.

In the SMER network, for example, a dense distribution of network devices and the diversity of their characteristics cause performance problems. The contention increases as more network devices are deployed into the field. The diversity in energy consumption and power supply makes the problem more complex. If the nodes with battery power contend with

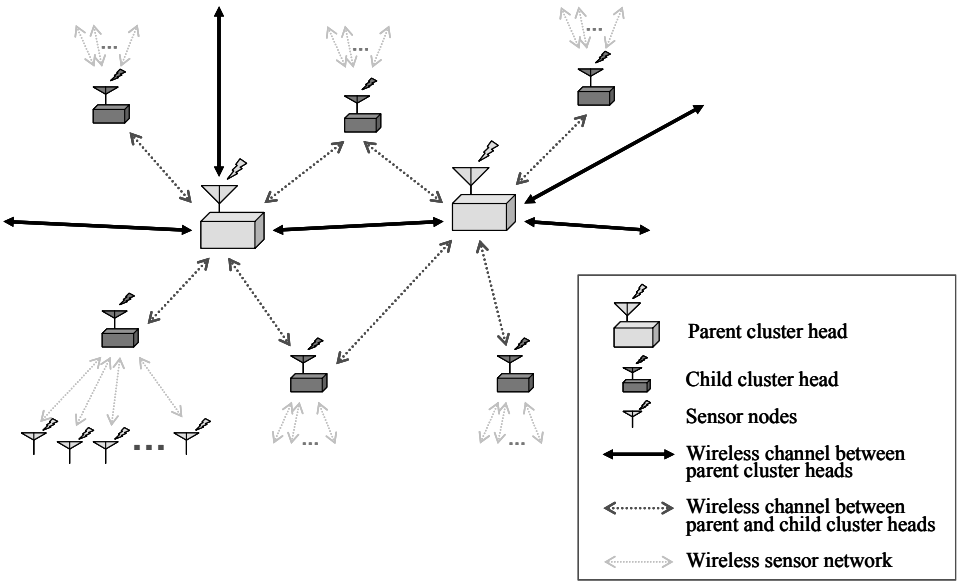

Figure 3. Structure of the heterogeneous wireless network composed of three layers

line-powered nodes and if the contention causes too many packet retransmissions, the batteries of the nodes can be exhausted quickly. If the network resources do not sufficiently satisfy all the requirements, applications suffer from low throughput, delayed arrival times, and other performance problems. Relaxing the network contention can lessen performance problems. By reducing the network contention between nodes, the number of packet retransmissions decrease, which results in lower communication power consumption. In addition, reducing conflicts in packet transmission often improves throughput. Therefore, we propose a novel distributed scheduling algorithm to drastically lower power consumption and to improve network performance at the level of child cluster heads.

The most important goal of our scheduling algorithm is to reduce the energy consumption of the child cluster head nodes. We decrease communication power by switching the nodes into a sleep mode when they are not scheduled. This means that a node cannot communicate with other nodes while it is not scheduled. Most of QoS scheduling algorithms

for wireless networks use feedback or notifications from adjacent nodes at runtime. In that case, they require that the network interface is always active (turned on). For example, Overlay MAC in [28] successfully implements the distributed scheduling of 802.11 wireless nodes. The Overlay MAC, however, depends on a timer expiration mechanism to detect the idleness of a wireless channel. If we intend to save energy in communication devices, it is not easy to rely on timer expirations in the MAC layer. In heterogeneous wireless sensor networks, battery-powered wireless nodes need to put their wireless interfaces to sleep for a long time because power saving is a main concern in this type of wireless network. For this reason, the distributed scheduling algorithms we have developed are designed to work even if a network interface is not always active.

The goal of the scheduling algorithm presented in this thesis is to increase the battery lifetime of wireless nodes while maximizing the efficiency of bandwidth utilization in a hierarchical heterogeneous wireless sensor network. For this goal, we run a hybrid distributed scheduling algorithm that consists of two scheduling parts. At a cell level, we choose *active* cells that do not interfere with other scheduled cells. We allow only the nodes in scheduled active cells to access a wireless channel. At a node level, we control the number of nodes simultaneously accessing wireless media. The node-level scheduler decides which nodes in active cells are allowed to access the media.

To simplify the problem and to effectively target the layers with the most significant performance issues, we focus on the middle layer of the heterogeneous wireless networks; child cluster heads and parent cluster heads. We assume that appropriate scheduling and routing algorithms handle data delivery from sensors to a child cluster head in the lower layer. Child cluster heads deliver the collected sensing data to their parent cluster heads. Parent cluster heads form a mesh network by connecting to each other.

Our proposed scheduling algorithm runs in a *proxy* layer. The scheduler resides between OS kernel and user applications. The proxy is transparent to the applications running on the wireless nodes. For applications, the proxy layer is very similar to kernel protocol layers. Since legacy applications do not have to recognize its existence, they can work over the proxy layer with minimum modification. In addition, proxy layer implementation over transport/network layers does not require modifying MAC or kernel protocol implementation. Thus, the scheduling in the proxy layer is not dependent on the physical mechanism of wireless network systems. Therefore, our approach is very flexible and applicable to different types of wireless networks. In simulation results, we see a throughput improvement of up to 10.31% and maximum power saving of 85.54%.

The remainder of the thesis is organized as follows: we summarize the related work in the next chapter. Motivations for this research are introduced in Chapter III. Our new scheduling algorithms are presented in Chapter IV. In Chapter V, the simulation setup and the simulation results for our scheduling algorithm are presented. Finally, we conclude our discussion in Chapter VI.

II. RELATED WORK

There has been a significant amount of research on performance and quality of service (QoS) of wireless networks. The research on throughput degradation explains why and how packet collisions affect throughput in wireless networks. Many scheduling algorithms have been developed to improve throughput, to reduce energy consumption in communication, and eventually to provide a better framework for meeting requirements for QoS.

The problem of throughput degradation in a wireless network has been investigated in detail. In [17], the maximum theoretical bandwidth is calculated from the given MAC scheme, MSDU size, modulation scheme, and data rate. In the actual networks, however, there are multiple wireless nodes. The interaction and interference between nodes prevent the network from achieving its maximum bandwidth. As the number of contending nodes increases, the aggregate throughput falls gradually because collisions between nodes happen more frequently and the backoff time increases due to a longer contention window [14]. This performance degradation becomes even worse in real networks [8] [36] because 802.11 MAC lowers its transmission rate according to the channel quality. This may cause severe performance degradation.

Many algorithms have been proposed to solve the performance degradation problem in wireless networks. The first approach to this problem is to revise MAC layer algorithms. The original DCF algorithm cannot give prioritized service to user. Enhanced DCF (EDCF) [22] prioritizes traffic categories with different contention parameters. According to the priorities, a wireless node can implement up to eight transmission queues. Each transmission queue has different parameters for deciding its backoff time. With this, EDCF gives more chance of channel access to high priority traffic. EDCF is compatible with legacy DCF while

providing a differentiated service. The Distributed Fair Scheduling (DFS) in [35] differentiates the backoff interval (BI) according to the packet length and traffic class. As the node with the smallest BI transmits packets first, DFS enables the service differentiation by adjusting BI values. The Opportunistic Auto Rate (OAR) protocol in [31] exploits the automatically adjusted transmission rate of 802.11. The OAR protocol sends multiple back-to-back data packets when the channel quality is good. To enable this, it changes the information fields in RTS/CTS packets to send more data packets in a reserved transmission time slot. All the algorithms in this category require modifying the existing DCF mechanism or the packet headers. Therefore, it is very difficult to apply the above algorithm to the existing network devices.

Other work has focused on scheduling over the MAC layer, which means that legacy network devices can be used. Overlay MAC in [28] adds an additional conceptual layer over the existing 802.11 MAC. By allowing only one host to access wireless media for a time slot, Overlay MAC alleviates the unfairness problems including the throughput imbalance between asymmetric sender transmit rates. The authors extend this idea to a multi-hop wireless network. Its merit is that Overlay MAC is implemented over the off-the-shelf 802.11 MAC layer and requires just a few assumptions on the MAC interface. However, Overlay MAC depends on the idle-timer mechanism in order to detect idle time slots not used by other nodes. Therefore, all nodes in a network must keep their network interfaces turned on, which makes it difficult to achieve energy saving. SWAN [4] is a rate control mechanism for TCP and UDP traffic which works on the best-effort MAC, not requiring any support for a QoS-capable MAC. SWAN provides service differentiation and sender-based admission control. Its rate controller resides between the IP layer and the MAC layer, while the admission controller works over the IP layer. The strength of SWAN's model is that it is a distributed mechanism and works

with feedback from the network. It collects the feedback information from the MAC layer or from other network nodes. SWAN improves throughput and achieves good fairness among different traffic. However, it does not consider the energy consumption of wireless nodes.

In the previous research on scheduling at the MAC layer, the main goal is to improve the overall performance of the whole network by achieving fairness among wireless nodes. The research in Overlay MAC and SWAN assumes that nodes continuously listen to a channel. Energy consumption of mobile nodes is not considered in their work. In our research, we combine scheduling with power management. Because mobile nodes do not need to keep listening to the channel, they can turn off their radio devices for a period of time. In this way, we obtain both large power savings and an additional throughput gain due to decreasing contention.

Work presented in [11] combines scheduling and power control. They have two phases in their cross-layer framework. First, the scheduling algorithm coordinates nodes' transmissions to eliminate strong interference. Next, scheduled nodes control the radio power while satisfying the given noise constraints. Basically, their algorithm performs the distributed transmit power control while scheduling wireless nodes. The problem is that their mechanism requires a separate contention-free feedback channel for sending information about radio conditions. Furthermore, their scheduling algorithm is not fully distributed because it runs on a central controller node. In our research, we use only one radio channel, and each node determines its schedule by running the scheduling algorithm itself.

Distributed scheduling is an important part of our research. Centralized scheduling is vulnerable to the failure of the single control node. There has been research on running distributed scheduling algorithms on wireless networks. The protocol in [25] coordinates the assignment of exclusive time-slots among neighboring nodes. In this algorithm, all nodes in a

network are assumed to have tight timing synchronization. Another distributed scheduling algorithm in [27] first forms a depth-first-search (DFS) tree from nodes by exchanging a token throughout the network. Then, it establishes a schedule table of nodes from the constructed DFS tree. The application-adaptive scheduling on overlay wireless sensor networks [37] provides fairness among applications with different bandwidth requirements. To exchange the feedback of traffic quality and the control messages, it uses a two-tier network that additionally includes a control channel with lower bandwidth. Although these algorithms work in a distributed way, they assume a special framing of radio channels [25], a separate radio channel [37], or the traversal of the entire network using a special token [27]. On the contrary, we present a fully distributed algorithm which works at each node using partial knowledge of the whole network. Our algorithm requires only the information of nodes within one- or two-hop distance. It requires very little runtime overhead. The overhead only occurs when a new node enters the network. In this case, a new node broadcasts its unique node ID to neighbor nodes and gets the node IDs of its neighbors. The number of packet transmissions for setting up a new node is proportional to the number of neighboring nodes.

Another distributed power scheduling algorithms is presented in [15]. Their technique performs distributed power management on demand of applications, in which radio devices are turned off during idle slots. The authors provide a two-level architecture for combining the management of power control and channel access. Their main goal is to save power of sensor nodes while providing a trade-off between energy saving and latency. In our research, we also focus on saving communication power while managing latency. Our research is different as we also improve the network capacity in aggregate throughput. Since the scheduling algorithm proposed in this thesis runs on cluster head nodes over sensor networks, it is possible to combine our scheduling with the existing scheduling algorithms on the underlying sensor

networks.

Maximizing network capacity, while reducing interference between wireless nodes, is a long-standing issue in multi-cell wireless networks. When a network consists of multiple cells, a channel assignment scheme increases the capacity of the network throughput by allocating different radio channels to adjacent cells. However, the limited availability of radio channels makes channel assignment a challenge. The channel assignment problem in multi-cell networks has been shown to be equivalent to a graph-coloring problem in [13] and [29]. On a given channel, the problem of maximizing the limited capacity of aggregate throughput has been studied extensively. One solution is to control the transmit power of wireless interface devices shown in [43]. A transmit power control scheme is effective in maximizing the number of simultaneous connections in a network channel. However, the accurate control of transmit power requires the access to network interface devices and the knowledge of signal power on physical/link layers. It is also common that the transmit power control scheme needs a separate feedback channel. The runtime overhead for delivering feedback information is not negligible. In this research, we do not use the transmit power control of wireless interface devices. Instead, we control the channel access of cells on a high level and the channel access of nodes on a lower level. In the proposed scheduling algorithm, only the scheduled nodes in the active cells are allowed to access the channel.

In order to run the proposed scheduling algorithm over kernel protocol layers, we use a proxy layer. In other words, our scheduling algorithm runs over the existing transport layer. In general, proxies are widely used for caching web traffic or multimedia data [42] [30] . Because of its adaptability to legacy systems, proxies are also used for frameworks supporting high-level traffic management, such as service differentiation of streaming traffic in [32]. The proxy provides transparency of interface to the applications. It is also easy to implement new scheduling policies in the proxy without modifying the implementation of lower layers.

III. MOTIVATION

In this chapter, we motivate our research. As explained in Chapter I, our research focuses on achieving power saving while providing higher network throughput capacity. Our target network, the SMER network in HPWREN [2], has IEEE 802.11 wireless connections between cluster head nodes deployed in the Santa Margarita Ecological Reserve. IEEE 802.11 is a good example of high speed wireless networks, and it is suitable for establishing connections among cluster heads. However, wireless channels between cluster heads often suffer from the lack of network throughput due to a large amount of data traffic collected from sensor nodes. In a typical multi-cell wireless network, performance degradation is caused by both contention between nodes and interference between cells. In the first section of this chapter, we summarize the underlying mechanism of IEEE 802.11 MAC, in particular its DCF access mode. In the next section, we examine the performance degradation problem caused by excessive contention between the nodes in a single-cell network. In the last section, we study the details of interference between neighboring cells.

1. IEEE 802.11 MAC

IEEE 802.11 defines two types of network service models. Independent BSS (Basic Service Set), called IBSS or *ad hoc network*, is composed of independent node stations. In IBSS, the nodes communicate directly with each other without an access point. On the contrary, an infrastructure BSS, commonly called *infrastructure mode*, uses an access point. In the infrastructure BSS, all wireless communication occurs between access points and mobile nodes. When a mobile node sends data to another node, data is delivered through an access point. Currently, the 802.11 infrastructure BSS is the more popular wireless network model in the market. In this thesis, all discussions about wireless network services refer to the

infrastructure BSS.

In 802.11 MAC, there are two well-known MAC access modes; a point coordination function (PCF) and a distributed coordination function (DCF). Even though PCF provides contention-free services, it is not widely implemented among 802.11 devices in the market. DCF uses the standard CSMA/CA access mechanism. It is possible to use the RTS/CTS technique with DCF to reduce the possibility of collisions. However, the RTS/CTS mechanism incurs overhead due to additional frame transmissions. Because of this overhead, the actual throughput in RTS/CTS mode is lower than it is without RTS/CTS. Therefore, use of RTS/CTS is usually limited to relatively long size packets. The threshold for RTS/CTS is set as a RTS threshold. In practice, almost all frames are limited to a size smaller than RTS threshold by the Ethernet MTU value or by TCP fragmentation. In most of practical wireless networks, the RTS/CTS mechanism is not widely used because of its overhead from additional packet transmissions. In this thesis, we do not use the RTS/CTS mechanism.

In the DCF mode, wireless nodes compete with others to access a wireless channel.

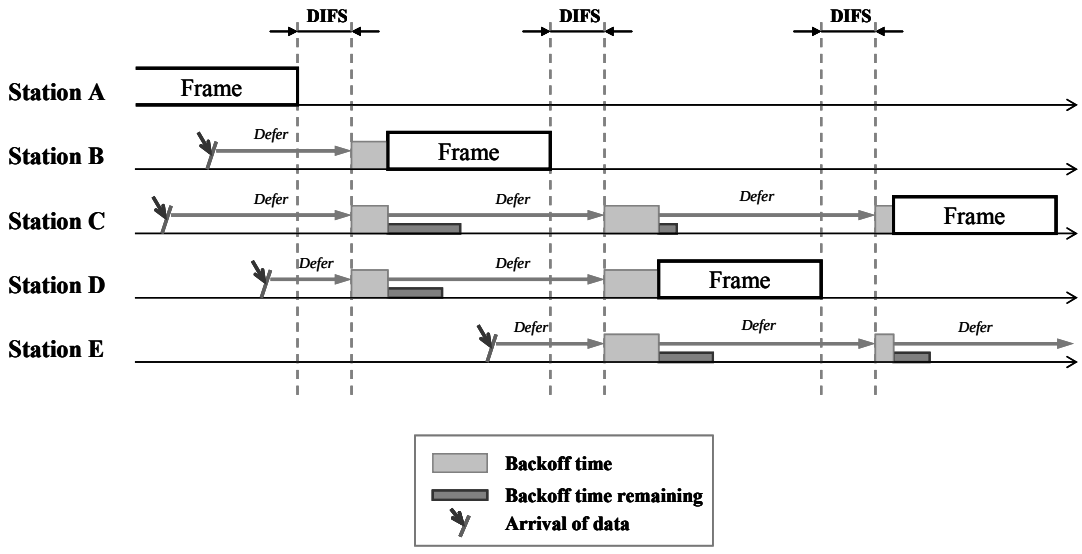

Figure 4. 802.11 DCF model

Before getting the right of access, a node waits for some time to check if any other nodes are accessing the channel. If other nodes are accessing the channel, all the other nodes that want to use the wireless media should wait for the channel to be idle. This is called *access deferral*. Access deferral does not end immediately after the channel becomes idle; however, it leaves an interframe space. The interframe space refers to an additional deferral after the transmission of a frame. To give different priority levels to frame types, interframe spacings vary among frame transmissions. Figure 4 shows how access deferral and interframe spacing work. For simplicity, only data frame type is drawn. In the actual 802.11 MAC, an ACK frame follows a data frame transmission. Interframe spacing between the data frame and the ACK frame is SIFS, which is shorter than DIFS.

In addition to deferral delay, 802.11 MAC includes another type of delay time to prevent simultaneous media access by multiple nodes. This delay is called *backoff*. Once the channel becomes idle, wireless nodes set a backoff timer. When the backoff timer expires, the corresponding node starts to transmit a packet through the channel. Backoff timers are suspended while other nodes access the channel or during access deferral. The length of a backoff time is determined by the Distributed Coordination Function (DCF) algorithm. DCF randomly chooses the backoff time in the range of contention window (CW) size. The backoff time is not a continuous value; instead, the contention window is divided into slots, and the backoff time is chosen from the divided slots. It is possible that two or more nodes try to access the channel at the same time slot if they choose the same backoff time, resulting in a *collision*. The 802.11 MAC algorithm requires an ACK frame to be sent back within a predefined expiration time. If the ACK frame is not received, the contention window is doubled and a new backoff time is chosen. The size of the contention window saturates at a predefined maximum value.

2. Performance degradation due to contention

When more wireless nodes are added into a network, there is a higher probability that nodes transmit packets at the same time, and they consequently cause more collisions. This leads to packet retransmissions and an increased CW size, which means that nodes could wait longer before accessing a wireless channel. Given that all nodes have data packets to send, MAC layer queues are always full. In that case, as there are more nodes in a wireless network, the chance of successfully transmitting a packet through the wireless channel decreases dramatically as the probability of collisions increases. In that case, nodes spend a lot of time waiting for the channel to become idle while no node can successfully transmit a packet. Therefore, the total aggregate throughput of a wireless network drops because the utilization of wireless channel decreases.

Figure 5 shows how much the aggregate throughput drops as the number of wireless nodes increases. In this simulation, we have one base station (access point) and a lot of wireless nodes around the base station. Wireless nodes generate UDP data traffic and send it to a base station. The total amount of generated traffic is set higher than the aggregate throughput, so that MAC layer queues are always full. We change the number of nodes in a network and measure the aggregate throughput at a base station. Similar results have been reported in [14] and [8]. Simulation results show that the throughput reaches its maximum when there are three nodes in the network, excluding the base station. As the number of nodes increases, the throughput drops gradually.

The maximum throughput measured in our simulation is 5.2Mbps. Many factors affect this number, such as packet size, traffic type, noise strength, error rate and the location of nodes. In the simulation, we use UDP traffic. Aside from traffic type, the most influential factor is the size of the payload, which is the length of application data in a packet. Generally,

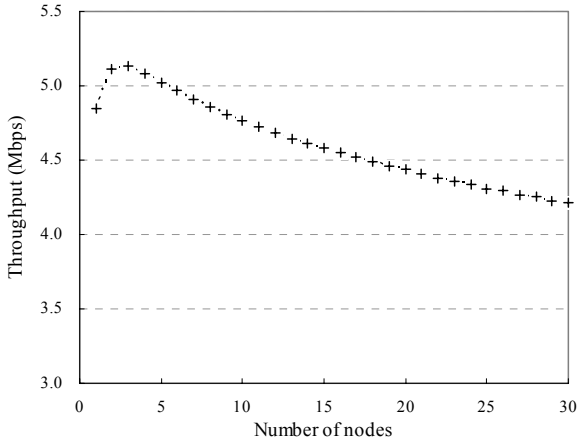

Figure 5. Aggregate throughput with different number of wireless nodes

as the size of an UDP payload increases, the portion of transmission overhead falls off as long as the size does not exceed the RTS threshold. The overhead includes the UDP header, MAC header, DIFS spacing time, and ACK frame transmission. Thus, the throughput gradually grows as the payload size increases until the size reaches the RTS threshold. Once the payload size is larger than the RTS threshold, the RTS/CTS mechanism is used and the overhead rises. In this simulation, we use a UDP payload size of 1000 bytes without the RTS/CTS mechanism.

In Figure 5, the aggregate throughput decreases gradually after reaching the maximum. A drop in the throughput can be accounted for the increasing number of collisions. As explained in the previous section, collisions in frame transmissions introduce a large amount of retransmissions and further defer the next trial of frame transmission.

The analysis of MAC layer performance is shown in Figure 6. Figure 6 (a) shows the percent of collisions for the total number of frame transmissions, including successful and failed transmissions of data and ACK frames. For example, when there are twenty nodes in a wireless network, more than 10% of packet transmissions suffer from collisions. The collision

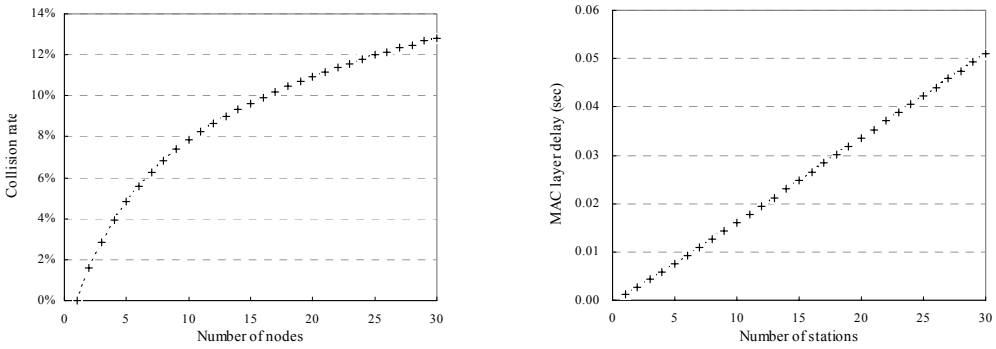

(a) Collision rate (b) Transmission delay

Figure 6. Congestion on MAC layer

rate increases steadily as more nodes join the network. If more collisions occur, they incur more retransmissions of data and ACK frames. We can expect that many collisions lead to longer packet transmission delay.

Figure 6 (b) represents the average transmission delay of a data packet on the MAC layer. The delay is measured only for successfully delivered packets. Here, the delay is defined as the time between when the data packet is taken out from a MAC-layer queue and when the MAC-layer ACK frame is received. If a packet is retransmitted due to collisions, the delay increases. In the typical MAC layer algorithm, a new packet transfer can only be started after the MAC layer finishes the transmission of the current packet or drops it. Thus, the longer transmission delay decreases the number of delivered packets in a fixed time slot, which translates to lower throughput.

From the simulation results, it is clear that we can get a higher throughput by limiting contention to only a few nodes at a time. For example, if there are twenty wireless nodes with full MAC-layer queues, a possible aggregate throughput is less than 4.5 Mbps. However, after restricting the number of competing nodes to three, the throughput can reach up to 5.12 Mbps, an improvement of 13.8%. In a wireless network where the low throughput has an impact on

performance, this improvement can help applications use network resources more effectively.

It should be noted that scheduling wireless nodes gives a large benefit in terms of energy consumption. While a node is not scheduled to participate in wireless communication, the node can be switched to a low-power mode. This reduces power consumption of wireless nodes. Furthermore, limiting the number of nodes that concurrently access the channel by scheduling reduces collisions and retransmissions of packets. This also helps in reducing the power dissipation.

In this section, we examined the performance problem due to contention between the nodes that are close to each other. Packet collisions by contention happen when multiple nodes transmit packets during the same backoff slot. In contrast, interference occurs when packet transmission of other nodes is deferred by a node transmitting data over the channel. In a large-scale network with multiple cells, nodes in neighboring cells of a transmitting node suffer from interference from the transmitter. Due to the wide range of carrier sensing, the effect of interference between cells is a dominating factor of the throughput degradation problem in multi-cell wireless networks. In the next section we study this interference issue in detail.

3. Interference in a multi-cell wireless network

Although a single-cell scheduling algorithm successfully reduces contention, it does not effectively reduce interference in a multi-cell network. This is because it does not consider interference from nodes in nearby cells. Even if single-cell scheduling reduces contention from neighboring nodes in the same cell, there is still a large amount of interference from other nodes in adjacent cells. Thus, active nodes do not have enough chance to access channels. Moreover, because of location differences, even the nodes in the same cell have different sets of interfering nodes. This difference often leads to the well-known hidden

terminal problem [20].

To explore how much the interference affects the throughput in multi-cell networks, we run the following simulations. In a multi-cell topology of 533m by 550m size, we locate 39 base stations in a hexagonal pattern. The topology used in this simulation is shown in Figure 19 (a) of Chapter V. The communication range of the radio is set to 50m. The carrier sensing range is twice as long as the communication range. Therefore, the radio signal of a node affects nodes in neighboring cells. In this setup, we measure the average throughput and MAC layer utilization at base stations. MAC layer utilization is defined as how much time the radio channel has consumed in each of MAC layer state. We focus only on two types of MAC layer states at base stations; *recv*, and *interference*. If a base station is receiving a packet and if the packet data is not corrupted, it is in a recv state. If a base station fails to receive an uncorrupted packet because of radio signals from more than one node, the node is in an interference state. Interference is different from collisions. While collisions are defined as the coincidental use of a backoff slot by multiple nodes, interference is caused by a hidden terminal. The other MAC layer states consume a minor portion of simulation time; less than 8% each. Thus, we do not consider the other MAC layer states in this analysis. Data traffic used in this simulation is UDP upstream from child nodes to the closest base stations. The data rate from child nodes is set to be higher than the maximum throughput. Therefore, MAC layer input queues at nodes are always full.

In this simulation, we run only the centralized node-level scheduling algorithm (CNLS) presented in the next chapter. Briefly, its strategy is to randomly choose a given number of nodes within a communication range. In the following simulation, we schedule only four nodes within a communication range. Only the scheduled nodes are allowed to access the channel. This node-level scheduling reduces packet collisions. Therefore it is very

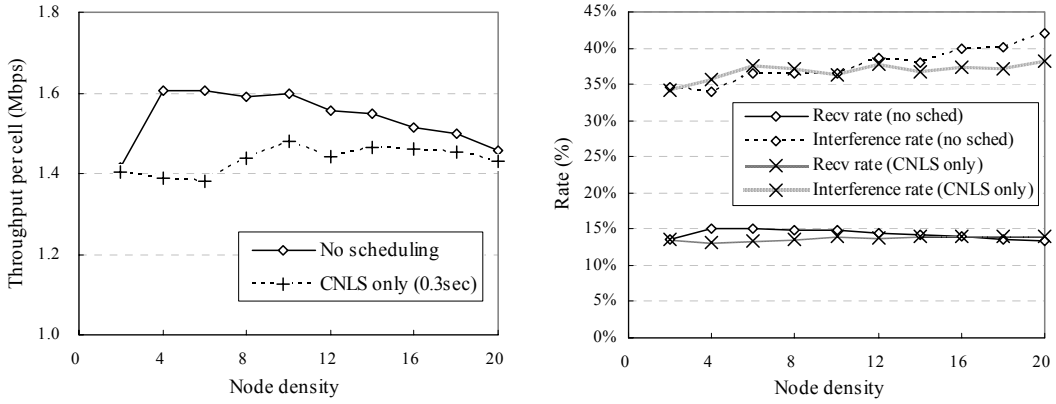

(a) Aggregate throughput (b) Recv/interference rate

Figure 7. Measurement of throughput and interference in a multi-cell wireless network

effective in improving the throughput in a single-cell wireless network [21].

Figure 7 (a) shows the measured result on the average throughput at base stations. In this figure, the node density is defined as the average number of child nodes in the circle area of the communication range. In the previous research [21], the node-level scheduling is very helpful in improving the throughput by reducing packet collisions. However, from the result in Figure 7 (a), it is found that running only the node-level scheduling algorithm is not helpful to improve the throughput in multi-cell networks. We can find the reason from the analysis in Figure 7 (b).

Figure 7 (b) shows how much simulation time is consumed in the recv and interference states. In the figure, we find that only 15% of time is used for communication. More than 35% of time is wasted by interference, mostly from hidden terminals. Although the node-level scheduling lowers the interference rate, it is not effective in improving the recv rate. Though packet collisions are already reduced to less than 1.5% by the node-level scheduling, the interference rate is still very high, more than 35%. Thus, the throughput drop in a multicell wireless network is largely due to the interference from the neighboring cells. Therefore, our

scheduling algorithm needs to consider both contention within a cell and interference from neighboring cells.

IV. SCHEDULING ALGORITHM

In this chapter, we study an optimal and a heuristic scheduling algorithm for multi-cell wireless networks, and compare them with our distributed scheduling algorithms. We also explain our scheduling algorithm in detail.

The wireless network we consider consists of three layers as shown in Figure 8. It is representative of real heterogeneous wireless networks such as HPWREN [2]. The top layer is a high-speed wireless mesh network between parent cluster heads (CHs). The middle layer is a 802.11 wireless network working in infrastructure mode, where each group of close child cluster heads connects with a parent cluster head. The lowest layer is a typical sensor network, through which sensor nodes reach nearby child cluster heads. We target our research to the middle layer. A child cluster head node is referred to as a *node* when discussing the network topology.

Data communication between parent cluster heads and child cluster heads occurs via

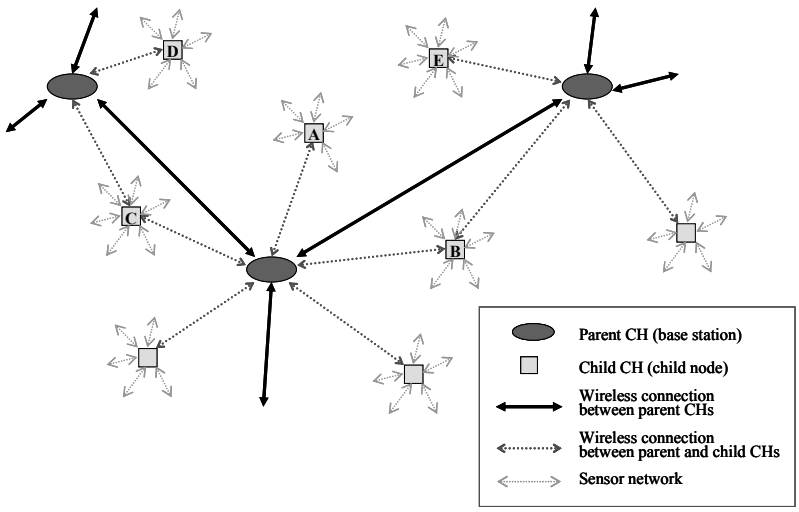

Figure 8. The architecture of a heterogeneous wireless network

the contention-based MAC mechanism. As a result, contention and interferences are issues. To handle these problems, we first define *neighbor* nodes as the nodes within communication range from a target node. Neighbor nodes of Node *A* can receive the packets from Node *A* in a promiscuous mode of the wireless interface. It is possible to get an unique ID for nodes by reading the source address of packets. Therefore, we assume that a node knows the existence and the unique node IDs of its neighbor nodes.

Once a node finds its neighbor nodes, it can construct a *contention graph* as the one shown in Figure 9. The contention graph in Figure 9 is built from the child cluster heads in Figure 8. A contention graph consists of nodes and links between them. An edge between two nodes means that they are neighbor nodes of each other. A node contends with its neighbor nodes for channel access. For example, Node *A* has four neighbor nodes in Figure 9.

Lower energy consumption is also an important goal. We put the wireless communication device of a node into a *sleep* mode when the node is not scheduled for

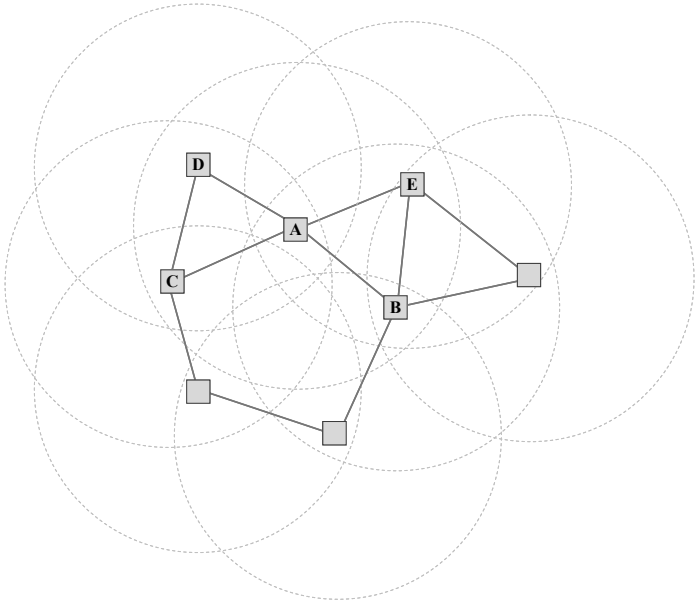

Figure 9. Contention graph constructed from Figure 8

communication. A node in a sleep mode is called *inactive*. When an inactive node turns its wireless interface back to a *ready* mode, it becomes *active*. Of course, the mode transition from the ready mode to the sleep mode or vice versa requires energy higher than in a sleep mode, as well as the mode transition time.

Our algorithm consists of two parts; cell-level scheduling and node-level scheduling. These two algorithms schedule active cells and active nodes in scheduled cells respectively. Once the nodes are scheduled, they are active in the corresponding *scheduling interval*. The scheduling interval is a fixed period of time in which a schedule determined by the scheduler is valid. Our scheduling algorithm is based on a TDMA scheme. At the end of the scheduling interval, the cell-level scheduling algorithm decides new active cells, and the node-level scheduling algorithm chooses active nodes in these active cells.

The following sections of this chapter describe our scheduling algorithm in detail. In the first section, we define the node-level scheduling problem. We show that the optimal solution for the problem is NP-complete. Because it is very costly to run the algorithm for the NP-complete problem in a large-scale network at every scheduling time interval, in the next section we present another heuristic algorithm for the node-level scheduling problem. This algorithm is then generalized so that it runs in the distributed manner. Finally, we develop a distributed algorithm that uses both node-level and cell-level scheduling.

1. Optimal node-level scheduling

In this section, we define the node-level scheduling problem. Then we present the optimal scheduling algorithm for the problem. We also show that the optimal algorithm is NP-complete. Because it is not practical to repeatedly run an NP-complete algorithm in a large-scale wireless network, we provide a heuristic solution for the same problem in the next section.

As explained in Section III.2, the wireless MAC suffers from excessive contention when there are many nodes in a network. The maximum throughput is achieved only when the number of contending nodes is limited. The node-level scheduling problem in a contention-based wireless network can then be defined as scheduling at most *s* nodes in a given time slot around the contention range of any active node.

Given a network topology of *n* nodes, we define a contention graph $G=(V,E)$ as shown in Figure 9. A set of vertices *V* represent the nodes, and a set of edges *E* represent the *neighbor* relationship between the nodes. If a node $v_i \in V$ is a neighbor of the other node $v_j \in V$, then $(v_i, v_j) \in E$. The output of a scheduler is an assignment of nodes that are allowed to access the wireless channel in a given scheduling interval. An *active node* is a node which is scheduled to access the wireless channel. Thus, the scheduled assignment is a set of active nodes *AV,* where $AV \subseteq V$.

The main constraint in the node-level scheduling problem is that the number of neighboring active nodes should not exceed a given constant ***s***. Let $N(v_i)$ be a set of neighbor nodes of $v_i \in V$. At v_i, let the set of active nodes which are in $\{v_i\} \cup N(v_i)$ be $AV(v_i)$. In other words, $AV(v_i)$ is a set of active nodes that are either v_i or neighbor nodes of v_i. Then, the set of all active nodes in a network is $AV = \bigcup_{v_i \in V} AV(v_i)$. In the constraint definition below, we note that $|A|$ means the number of elements in the set *A*.

$$\text{Constraint} \;:\; \forall v_i \in V,\; |AV(v_i)| \le s \;\text{ where }\; |AV(v_i)| \text{ is the number of nodes in } AV(v_i) \qquad \text{- I.1}$$

In scheduling wireless networks, the optimal schedule assigns active nodes such that

the assignment maximizes the size of AV. This assignment is called *maximum assignment*. In terms of the number of active nodes in a given network, maximum assignment is optimal. On the other hand, *maximal assignment* is to schedule the nodes so that the number of active nodes is maximal. By maximal we mean that no additional assignment of an active node to an existing schedule can meet Constraint I.1. The maximal assignment problem is simpler than the maximum assignment and it can be solved in polynomial time. The output of maximal assignment is dependent on the order of scheduled nodes. The number of active nodes in a maximal assignment is equal to or less than that of a maximum assignment.

It has been shown in [5] and [9] that the maximum assignment problem for $s = 1$ is NP-complete. Maximal assignment requires less computation than the maximum scheduling. We show that the maximum assignment problem for $s > 1$ is also NP-complete. We argue that scheduling the maximal assignment of nodes is feasible for scalable wireless networks.

NP completeness of the maximum assignment for $s = 1$

It has been reported in [9] that the decision problem of whether there exists an assignment of t active nodes in a given network is equivalent to the maximum clique problem, which is an NP-complete problem. We briefly summarize it here.

In a network graph $G = (V, E)$ and a set of scheduled active nodes $AV \subseteq V$, any two adjacent nodes cannot be active at the same time because $s = 1$. In other words, if a node is active, all its neighboring nodes cannot be active.

$$\{v_i, v_j\} \not\subset AV \quad \text{if} \quad i \neq j \quad \text{and} \quad (v_i, v_j) \in E$$

We map a graph $G = (V, E)$ into the corresponding $G' = (V', E')$ as the following.

Vertices : $V' \leftarrow V$

Edges : $E' \leftarrow E' \cup \{(v_i, v_j)\}$ for $\forall i, j$ where $i \neq j$ and $(v_i, v_j) \notin E$

G' has the same nodes as G. Nodes v_i and v_j in G' have an edge between them if and only if v_i and v_j are not a neighbor node of each other in G. Then, the decision problem of scheduling *t* active nodes in *G* is equivalent to the problem of finding a clique of size *t* in G'. There exists one-to-one mapping between *G* and G'. The mapping takes polynomial time. The decision problem of maximum clique is known as NP-complete. Therefore, finding the maximum assignment for *s* = 1 is NP-complete.

An example for the conversion from *G* to G' is shown in Figure 10. Figure 10 (a) is a contention graph. It has eight nodes, and four of them have been scheduled. Scheduled nodes are shown in gray color. Now, this graph *G* is converted to the corresponding graph G' by the above conversion rules. In Figure 10 (b), the graph G' has the same number of nodes as *G*. But, because v_1 has edges with v_4 and v_7 in *G*, we link v_1 with the nodes other than v_4 and v_7 in G'. The maximum clique in G' is drawn with dark thick lines. The nodes belonging to the maximum clique are the active nodes scheduled in the maximum assignment.

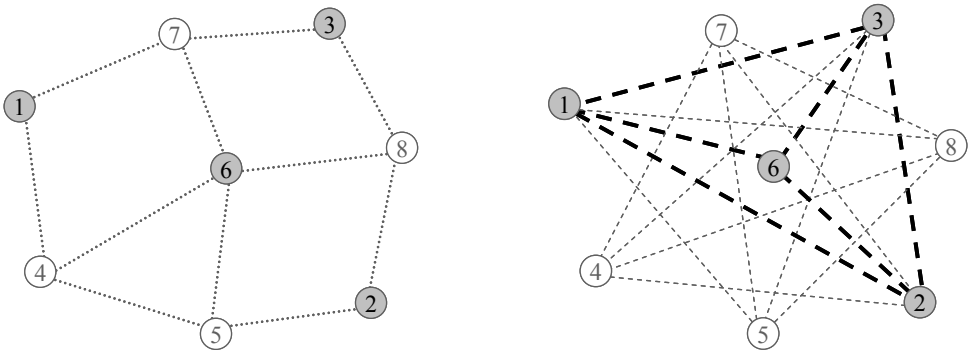

(a) $G = (V, E)$ (b) $G' = (V', E')$

Figure 10. Conversion from G to G' and the maximum clique of size 4.

NP completeness of the maximum assignment for $s \geq 1$

As far as we know, nobody has shown that the maximum assignment problem for $s > 1$ is NP-complete. Because we consider the scheduling problem for $s > 1$, it is important to show that this problem is NP-complete. If it is NP-complete, maximum scheduling cannot be scalable over a large-size network. However, maximal scheduling would be a feasible solution if it performs close to maximum scheduling. To show that the maximum assignment problem for $s > 1$ is NP-complete, we extend the idea for $s = 1$ into the case for $s > 1$.

In a given network $G = (V, E)$, we define a corresponding graph $G' = (V', E')$ as the following. First, let $N(v_i)$ be a set of neighbor nodes of a node $v_i \in V$. Define $d(v_i)$ as the degree of a node v_i which is the number of edges at v_i. This means $d(v_i)$ is also the number of neighbor nodes of v_i. In other words, $d(v_i)$ is equal to $|N(v_i)|$. For each node $v_i \in V$, add corresponding subnodes $v_{i,1}, v_{i,2}, \ldots, v_{i,S_{s-1}(v_i)}$ to V', where $S_{s-1}(v_i)$ is the number of subnodes in V' for a node $v_i \in V$. A subnode in V' represents one of the cases where some of v_i's neighbor nodes are scheduled together with v_i. We explain it below in detail.

$S_{s-1}(v_i)$, the number of subnodes in V' corresponding to v_i in *V*, is the number of ways to choose $s-1$ nodes from $N(v_i)$. For example, when $N(v_1) = \{v_2, v_3, v_4, v_5\}$ and $s = 3$, $S_2(v_1)$ is $\binom{|N(v_1)|}{3-1} = \binom{4}{2} = 6$. In other words, $S_{s-1}(v_i) = \binom{d(v_i)}{s-1}$. However, in the case of $d(v_i) < s-1$, v_i and its all neighbor nodes can be scheduled together without violating Constraint I.1. In that case, $S_{s-1}(v_i)$ is 1. In summary,

$$S_{s-1}(v_i) \text{ is, } \binom{d(v_i)}{s-1} \text{ if } d(v_i) \geq s-1, \quad \text{or 1 if } d(v_i) < s-1 \qquad \text{- I.2}$$

Now, we connect the subnodes in G'. For a subnode $v_{i,u}$ where $1 \leq u \leq S_{s-1}(v_i)$, we define $N'_{s-1}(v_{i,u})$ as a subset of $N(v_i)$ with the size of at most $s-1$. If $u \neq w$, then $N'_{s-1}(v_{i,u}) \neq N'_{s-1}(v_{i,w})$. In other words, $N'_{s-1}(v_{i,u})$ is a set of neighbor nodes of $v_{i,u}$ in G'. Also, $N'_{s-1}(v_{i,u})$ represents neighboring nodes that are scheduled together with v_i. When $N(v_1) = \{v_4, v_5, v_6\}$ and $s = 3$, for example, $N'_2(v_{1,1}) = \{v_4, v_5\}$, $N'_2(v_{1,2}) = \{v_4, v_6\}$, and $N'_2(v_{1,3}) = \{v_5, v_6\}$. This tells us that we have three choices in scheduling v_1 and its neighbors; we can schedule $\{v_1, v_4, v_5\}$, $\{v_1, v_4, v_6\}$, or $\{v_1, v_5, v_6\}$.

In the above, $v_4 \in N'_1(v_{1,1})$ does not mean $(v_{1,1}, v_4) \in E'$, because $v_4 \in V$ but $v_{1,1} \in V'$. Rather, it means that $v_{1,1}$ is linked with a subset of subnodes of v_4. The actual connectivity between subnodes in V' is explained next. We describe the definition of edges in two steps.

1. For $(v_i, v_j) \in E$, $i \neq j$ in G

If $(v_i, v_j) \in E$ in G, we add edges between subnodes $v_{i,u}$ and $v_{j,w}$ according to the following rule.

$$\text{For } \forall (v_i, v_j) \in E \text{ and } i \neq j,$$
$$E' \leftarrow E' \cup \{(v_{i,u}, v_{j,w})\}$$
$$\text{iff } v_j \in N'_{s-1}(v_{i,u}) \text{ and } v_i \in N'_{s-1}(v_{j,w}) \text{ for } \forall u, v \text{ and } u \neq w$$

- I.3

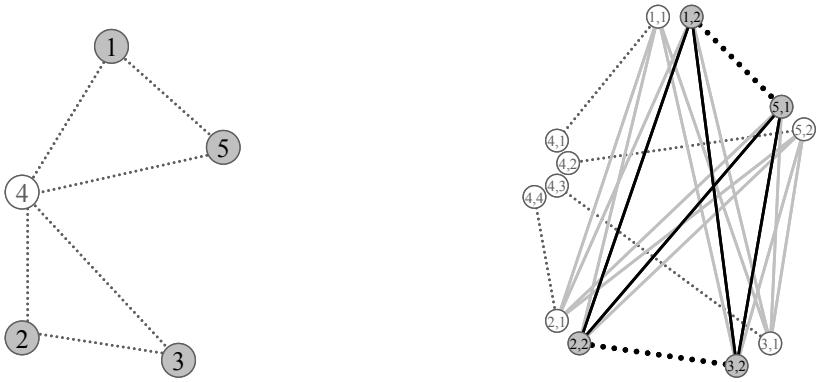

(a) $G=(V,E)$ (b) $G'=(V',E')$

Figure 11. Conversion from *G* to G', for *s* = 2

For example, in Figure 11, v_1 has an edge with v_5 in *G*. v_1 has two subnodes $v_{1,1}$ and $v_{1,2}$ in G'. v_5 also has two subnodes $v_{5,1}$ and $v_{5,2}$. Because *s* = 2, if a node is scheduled, we can schedule at most one of its neighbor node. So, $N'_{s-1}(v_{1,1})=\{v_4\}$ and $N'_{s-1}(v_{1,2})=\{v_5\}$. In the same way, $N'_{s-1}(v_{5,1})=\{v_1\}$ and $N'_{s-1}(v_{5,2})=\{v_4\}$. Now, we find that $v_5 \in N'_{s-1}(v_{1,2})$ and $v_1 \in N'_{s-1}(v_{5,1})$. Therefore, we place an edge between $v_{1,2}$ and $v_{5,1}$ by Rule I.3. The edges created by Rule I.3 are drawn with dashed lines in Figure 11.

2. For $(v_i,v_j) \notin E$, $i \neq j$ in *G*

$(v_i, v_j) \notin E$ means that v_i and v_j are not neighbor of each other. In this case, all subnodes of v_i can have links to subnodes of v_j. We can do this conversion by adding Rule I.4 to the definition of $N'_{s-1}(v_{i,u})$. Subnodes of v_i are then linked to subnodes of v_j by Rule I.3.

For $\forall(v_i, v_j) \in E$ and $i \neq j$,

$$N'_{s-1}(v_{i,u}) \leftarrow N'_{s-1}(v_{i,u}) \cup \{v_j\} \text{ and } N'_{s-1}(v_{j,w}) \leftarrow N'_{s-1}(v_{j,w}) \cup \{v_i\}$$

for $\forall u, v$ and $u \neq w$ - *I.4*

Rule I.4 means that any node v_j in *G* is added to $N'_{s-1}(v_{i,u})$ if v_j is neither v_i itself nor a neighbor node of v_i in *G*. For example, in Figure 11, v_2 and v_3 are not neighbor nodes of v_1. So, v_2 and v_3 are added to both $N'_{s-1}(v_{1,1})$ and $N'_{s-1}(v_{1,2})$. The edges created by Rule I.4 are drawn as solid lines.

When $s = 2$, the maximum assignment in Figure 11 is to schedule 4 nodes. We color the scheduled nodes as gray. Figure 11 (b) is a graph converted from Figure 11 (a). The maximum clique is shown with thick black lines. The size of a maximum clique is 4, so we can schedule up to four nodes.

Let the maximum clique found in G' be $MC(G') = (MV, ME)$. Then, we can derive the following facts from $MC(G')$:

Lemma 1 : If $v_{i,u} \in MV$ ***, then*** $v_{i,w} \notin MV$ ***for*** $\forall u \neq w$ ***- I.5***

Let us suppose that $v_{i,u} \in MV$ and $v_{i,w} \in MV$ for $u \neq w$. Then, there must be $(v_{i,u}, v_{i,w}) \in E'$, because $MC(G')$ is a maximum clique in G'. In a clique, there exist edges between all pairs of nodes. However, by the definition of a subnode and by Rule I.3 and Rule I.4, there cannot be any edges between subnodes derived from the same node. Therefore, $MC(G')$ includes at most one subnode for a node $v_i \in V$.

Lemma 2 : ***- I.6***

If there is a schedulable assignment of nodes in G ,

there exists a corresponding clique in G' .

When a given assignment of nodes is schedulable, it means $|AV(v_i)| \le s$ for $\forall v_i \in AV$. It is obvious that $|AV(v_i) - \{v_i\}| < s$ at any active node $v_i \in AV$. By the definition of $N'_{k-1}(v_{i,u})$, there must be at least one subnode $v_{i,u}$ satisfying $AV(v_i) - \{v_i\} \subset N'_{k-1}(v_{i,u})$. It is because subnodes of v_i cover all combinations of having $s-1$ neighbor nodes of v_i 's neighbors.

By the above, when two active nodes v_i and v_j satisfy $v_j \in N(v_i)$, it is always true that there exists a subnode $v_{i,u}$ of v_i and a subnode $v_{j,w}$ of v_j satisfying $(v_{i,u}, v_{j,w}) \in E'$. For v_i and v_j, if $v_j \notin N(v_i)$, then every subnode of v_i has edges with every subnode of v_j in G' by Rule I.4. Therefore, whenever a schedulable assignment of nodes is given in G , there exists a corresponding clique in G' .

Lemma 3 : ***- I.7***

If there is a clique in G' , there is a corresponding assignment of nodes in G .

By Lemma 1, the clique has at most one subnode for each $v_i \in V$. By the definition of Rule I.3 and of a maximum clique, a subnode $v_{i,u} \in MV$ has at most $s-1$ edges in $MC(G')$ with the subnodes of $N(v_i)$. So, any node $v_i \in V$ corresponding to $v_{i,u} \in MV$ does not violate Constraint I.1.

The assignment of nodes corresponding to $MC(G')$ is just to schedule the nodes

corresponding to MV ; for example, a schedule v_i if $v_{i,u} \in MV$ for any subnode $v_{i,u}$ of v_i . Obviously, the conversion from $MC(G')$ into the assignment in G takes $O(|V|)$ time.

Lemma 4 : Conversion of G into G' takes polynomial time. **- I.8**

Finding $N(v_i)$ for all $v_i \in V$ takes $O(|V| \cdot |E|)$ time. Rule I.3 takes $O(|V| \cdot |E|)$ time, and Rule I.4 needs $O(|V| \cdot |E|^2)$ time. Therefore, the conversion from G to G' takes polynomial time.

Theorem : The maximum scheduling problem is NP-complete. **- I.9**

By Lemma 2 and 3, there is an one-to-one mapping between the schedulable assignments in G and maximum cliques in G' . By Lemma 4, the conversion of a given network G to G' takes polynomial time. As shown in Lemma 3, it also takes polynomial time to map a maximum clique in G' into the schedulable assignment in G . We know that the maximum clique problem is NP-complete. Therefore, the given scheduling problem is-NP complete.

The goal of maximum scheduling is to maximize the number of scheduled nodes. On the other hand, maximal scheduling aims to schedule nodes until no more nodes can be scheduled. We showed that maximal scheduling problem is equivalent to the maximum clique problem which is known to be NP-complete. Running an NP-complete scheduling algorithm at every scheduling interval causes excessive runtime overhead. Therefore, in this research, we use maximal scheduling as a solution for determining the node-level schedule in a multi-cell wireless network. In the following sections, we present the centralized algorithm for maximal node-level scheduling. We next derive the distributed algorithm from the centralized version.

2. Centralized node-level scheduling (CNLS)

In this section, we first review the maximal node-level scheduling of a multi-cell wireless network for the case of ($s = 1$) where s is the maximum number of contending active nodes in a communication range. The algorithm for $s = 1$ has been presented in [9]. As explained in Section III.2 and III.3, we can achieve additional throughput gain and better utilization of radio channels by scheduling more than one node at a time. Furthermore, we extend the solution for $s = 1$ to the case of scheduling for $s > 1$ in a latter part of this section. We also note that the node-level scheduling algorithms presented in this section and the next section use a pseudo-random numbers generated with a seed value of node ID. Therefore, it is possible for each node to generate the identical set of pseudo-random values for all nodes. This eliminates runtime overhead of distributing a schedule to remote nodes at every scheduling interval.

Maximal assignment provides a deterministic node-level schedule when the network topology is known in advance. By deterministic, we mean that the algorithm for maximal assignment always gives the same assignment of active nodes if the order of pseudo-random numbers is fixed. Because the algorithm requires the complete knowledge of network topology, we say that this algorithm runs in a *centralized* manner. In contrast, the distributed node-level scheduling presented in the next section gives maximal assignment only with the knowledge of local topology. Therefore, it is possible for each node to run the distributed node-level scheduling algorithm. We first study the centralized node-level scheduling in this section, and convert it into a distributed version in the next section.

The centralized node-level scheduling algorithm (CNLS) for maximal scheduling based on [9] is shown in Algorithm I.10. The algorithm first chooses a node from vertices *V*, and schedules the node to the assignment of active nodes. Then the scheduled node and its

Centralized node-level scheduling algorithm for $s = 1$ **- I.10**

1. Pick a node $v_i \in V$ in the increasing order of pseudo-random numbers of nodes.
2. Add v_i to the assignment, $AV \leftarrow AV \cup \{v_i\}$
3. Remove v_i and its neighbors from V, $V \leftarrow V - (\{v_i\} \cup N(v_i))$.
4. If V is empty, then stop. Else go to 1.

neighbor nodes are removed from *V*. This is repeated as long as *V* is not empty.

Figure 12 shows an example of a maximal assignment schedule. For simplicity, we suppose that the increasing order of pseudo-random numbers of nodes is identical to the order of node IDs. Scheduled nodes are drawn with gray color. The algorithm picks up the nodes in the order of v_1, v_2, and v_3. Once v_1 is chosen and is scheduled, v_1 and its neighbor nodes v_5 and v_{11} are removed from *V*. The next node to be chosen is v_2. After v_2 is scheduled, we remove v_2 and its neighbors v_4, v_8, and v_{12}. In the same way, we schedule v_3. But, we cannot pick up v_4 because v_4 has been removed when v_2 was scheduled.

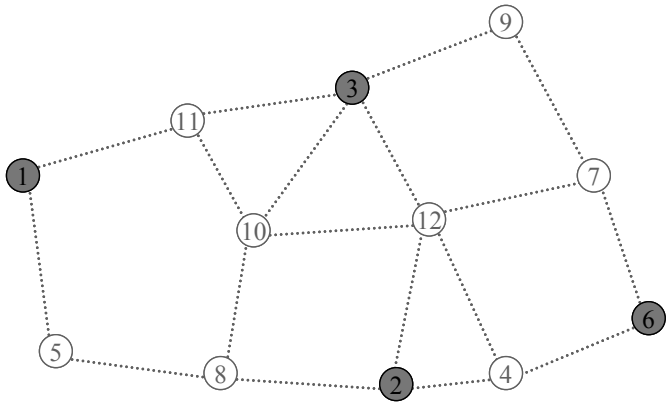

Figure 12. Maximal time slot assignment, *s* = 1

Hence, we choose the next available node v_6. After v_6 is scheduled, there is no more node to choose. Then, the algorithm terminates.

We next consider the case with more than one contending nodes within communication ranges ($s > 1$). In Algorithm I.10, the scheduled node v_i and its neighbors $N(v_i)$ are deleted from a node set V because both v_i and its neighbors already have one active node in their communication range. To guarantee the schedule to the case of $|AV(v_i)| > 1$, we assign s *tickets* to each node. The number of initial tickets in each node is equal to a constant s given in a scheduling constraint. The number of tickets at v_i limits $|AV(v_i)|$, the maximum number of active nodes at v_i. In this way, we limit the number of

Centralized node-level scheduling (CNLS) algorithm for $s \geq 1$ - I.11

1. Initialize the tickets of nodes, $tk(v_i) \leftarrow s$ for $\forall v_i \in V$.
2. Add all nodes into a set of unchecked nodes, $V'' \leftarrow V$.
3. Pick a node $v_i \in V''$ in the increasing order of pseudo-random numbers of nodes.
4. Determine if v_i can be scheduled. v_i is schedulable iff $tk(v_j) \geq 1$ for $\forall v_j \in \{v_i\} \cup (N(v_i) \cap AV)$
5. If v_i is schedulable, add it to the assignment of active nodes, $AV \leftarrow AV \cup \{v_i\}$. And decrease the tickets of v_i and its all neighbors by 1, $tk(v_j) = tk(v_j) - 1$ for $\forall v_j \in \{v_i\} \cup N(v_i)$.
6. Remove v_i from V'', $V'' \leftarrow V'' - \{v_i\}$.
7. If V'' is empty, then stop. Else go to 3.

contending nodes. For example, if a node has three tickets, we can schedule up to three nodes from the node and its neighbors. Let the current number of ticket at v_i be $tk(v_i)$. Note that $tk(v_i)$ may be negative if v_i is not scheduled in a given scheduling interval. Whenever the algorithm runs at every scheduling interval, $tk(v_i)$ is initialized as $tk(v_i) = s$. The new algorithm is shown in Algorithm I.11.

The new algorithm initially allocates *s* tickets to all nodes. If the number of active nodes near an unscheduled node v_i is equal to or greater than *s*, the number of tickets at v_i cannot be greater than zero, $tk(v_i) < 1$. Therefore, we do not schedule v_i because v_i already consumed its tickets. Otherwise, v_i is scheduled. In either case, we remove v_i from V''. The algorithm terminates if there is no more node to pick up from V''. By step 4 of Algorithm I.11, the new algorithm guarantees that, at any *active* node, the number of active nodes does not exceed the given constant *s*.

An example for *s* = 2 is given in Figure 13. Such as in Figure 12, we suppose that the node with a lower node ID has a lower value of pseudo-random number. The network topology is the same as the graph in Figure 12. In Figure 13, Algorithm I.11 first schedules

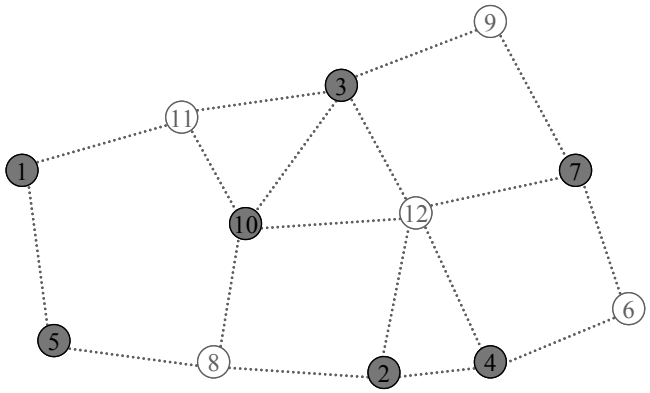

Figure 13. Maximal scheduling, *s* = 2

v_1. After v_1 is scheduled, the number of tickets at v_1, v_5, and v_{11} is decreased by 1. As a result, we get $tk(v_1)=1$, $tk(v_5)=1$, and $tk(v_{11})=1$. In the same way, v_2, v_3, v_4, and v_5 are scheduled. When we try to schedule v_6, we find that one of active neighbor nodes of v_6 has no remaining ticket, $tk(v_4)=0$. Hence, v_6 cannot be scheduled. However, v_6 can be scheduled even if the neighbor node v_{12} has no ticket, $tk(v_{12})=0$. We only look at the number of tickets only at active nodes. In addition, It is obvious that when $s=1$, the CNLS algorithm in I.11 is identical to Algorithm I.10. Therefore we can say that Algorithm I.11 is valid for $s \geq 1$.

CNLS algorithm gives a maximal scheduling when the whole topology of a network is known. However, maintaining the topology information at every node will result in a lot of overhead at runtime. As the network grows into a large in scale, the size of the topology information and the execution time of algorithm will also increase. Therefore, we need to run the CNLS algorithm in a distributed manner. By distributed, we mean that each node runs the node-level scheduling algorithm on its own in order to decide its schedule at every scheduling interval. We present a distributed version of CNLS in the next section. The performance of both scheduling algorithms is analyzed in Chapter V.

3. Distributed node-level scheduling (DNLS)

In this section, we present a distributed node-level scheduling (DNLS) algorithm for maximal scheduling. The CNLS algorithm in Algorithm I.11 of the previous section runs with the knowledge of the whole network topology. In a practical wireless network, however, it is not easy to share the complete network topology among all wireless nodes in a network. To update the topology information at all nodes whenever a new node joins the network requires high overhead in running-time and communication. Running the CNLS algorithm at every

Distributed node-level scheduling (DNLS) algorithm for $s \geq 1$ - I.12

1. Construct a subnetwork $G_i = (E_i, V_i)$

   a) Add the node v_i and its neighbors $N(v_i)$ into a set of vertices V_i,

   $V_i \leftarrow \{v_i\} \cup N(v_i)$.

   b) Add all neighbor nodes of v_i and its neighbors $N(v_i)$ into V_i,

   $V_i \leftarrow V_i \cup N(v_j)$ for $\forall v_j \in \{v_i\} \cup N(v_i)$.

   c) Add edges into E_i if the two end nodes of an edge are in V_i,

   $E_i \leftarrow E_i \cup \{(v_j, v_k)\}$ satisfying $(v_j, v_k) \in E$ for $\forall v_j, v_k \in V_i$

2. Run CNLS algorithm in I.11 on a subnetwork $G_i = (E_i, V_i)$

node is also redundant. Each node is interested only in its own schedule. Our distributed node-level scheduling algorithm addresses all these issues.

We first define the input to the distributed algorithm. In the centralized algorithm (Algorithm I.11), its input is the network topology; a contention graph. In a distributed scheduling algorithm which we present here, we use a partial knowledge of the network topology. We call this partial network topology a *subnetwork*. The size of a subnetwork is an important factor in determining accuracy and efficiency of our DNLS algorithm. For example, let us think of running DNLS with a subnetwork of one hop distance nodes. Each node runs Algorithm I.11 only for a subnetwork that includes the node itself and its neighbor nodes. However, because the schedule of a node is dependent on the schedule of its neighbor nodes, we cannot guarantee that the schedule resulting from the knowledge of subnetwork is always consistent with the result of the original CNLS for a total network. On the other hand, increasing the size of a subnetwork creates large overhead at runtime. Even a small change in the network topology propagates to a number of nodes, and the overhead increases

exponentially as the subnetwork grows. We use the subnetwork size of *two-hop distance* in our distributed node-level scheduling. The two-hop distance is a reasonable range because it does not incur much of runtime overhead while partially reflecting the influence of cascaded dependency over multiple hops. The performance of the scheduling with a two-hop subnetwork is evaluated in Chapter V.

The DNLS uses the CNLS algorithm described in Algorithm I.11. The only difference is the input to the algorithm. In CNLS, the input is a contention graph for the whole network topology. DNLS runs over a subnetwork of a node v_i. The subnetwork $G_i = (E_i, V_i)$ is a

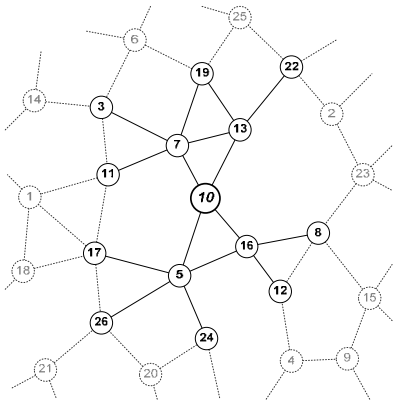

(a) A part of the original network topology

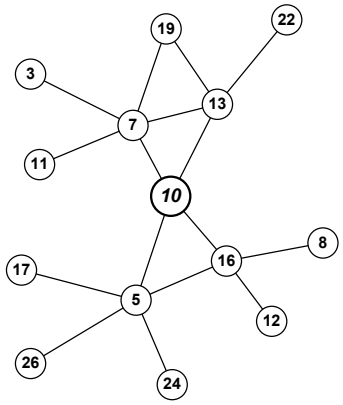

(b) A subnetwork within two-hop from v_{10}

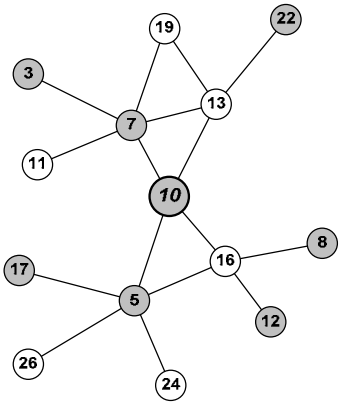

(c) Scheduled nodes after running CNLS

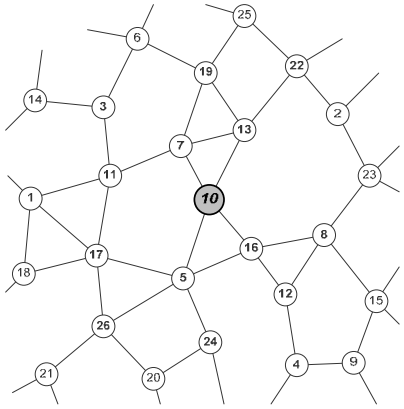

(d) Scheduling v_{10} at the original network

Figure 14. Example of running DNLS at v_{10}

subset of $G=(V,E)$. All vertices and edges within two hops distance from v_i are added to the subnetwork $G_i=(E_i,V_i)$. Once a subnetwork is created, we run the CNLS algorithm only on this subnetwork. The result of the CNLS algorithm becomes the schedule of v_i. We present the DNLS algorithm in I.12. At the last step of I.12, the schedule of v_i is determined by running CNLS algorithm on $G_i=(E_i,V_i)$.

Figure 14 shows an example of constructing a subnetwork and running the DNLS at a node v_{10}. In Figure 14 (a), the node v_{10} has four one-hop neighbor nodes and nine two-hop neighbor nodes. We build a subnetwork consisting of 14 nodes in Figure 14 (b). This is a subnetwork $G_{10}=(E_{10},V_{10})$ for a node v_{10}. Next, we run the CNLS algorithm over this subnetwork. The result is shown in Figure 14 (c). Since we run this scheduling algorithm at v_{10}, we are interested only in the schedule of v_{10}. The result from running CNLS over the subnetwork says that v_{10} is scheduled. Thus, DNLS algorithm gives the result that v_{10} is scheduled. The DNLS algorithm is repeated by all nodes at every scheduling interval.

The distributed node-level scheduling algorithm for a maximal scheduling has been presented in this section. The DNLS algorithm runs over a subnetwork that is a part of the whole network topology. As each node needs to know of nodes within two-hops distance, the DNLS algorithm reduces a large amount of computational complexity and runtime overhead in communication. Therefore, we use DNLS algorithm as a node-level scheduling algorithm. In the next section, we consider the cell-level scheduling algorithm. In our complete scheduling algorithm, the node-level scheduling algorithm is combined with the cell-level scheduling algorithm.

4. Cell-level scheduling

Wireless nodes in a multi-cell network are exposed to interference from other nodes in the carrier-sensing range. The effect of interference from other cells has been discussed in Section III.3. Interference severely affects throughput in a large-scale multi-cell wireless network. The degree of interference is dependent on an actual network topology and the size of carrier-sensing range. When carrier sensing is sensitive, a node defers packet transmission more often because it senses much more radio activity. Channel utilization in the network drops further. Therefore, in designing a scheduling algorithm for multi-cell wireless networks, it is very important to reduce the interference from neighbor cells.

The purpose of cell-level scheduling is to reduce the interference between nodes in adjacent cells. Contention between nodes in the same cell is already managed by node-level scheduling. Cell-level scheduling decides the active cells such that only the child nodes in the active cells are considered in node-level scheduling algorithm. Any child nodes in the cells not scheduled by cell-level scheduling algorithm are not active in a given time slot.

We define a cell C_i in a given multi-cell wireless network topology as a set of a base station BS_i and child nodes that are connected to that base station. A structure of a cell is shown in Figure 15 (a). Let the communication range of the channel be d_t, and the carrier-sensing range be d_{CS}. The base station in the center of a cell is marked as *BS*.

We assume a multi-cell topology with a regular pattern of cells. Two examples are hexagonal topology in Figure 15 (b) and square topology in Figure 15 (c). These networks are constructed so that any child nodes in the fields are within d_t from at least one base station. d_{CS} is defined as a twice of d_t. In addition, we define neighboring cells of a given cell C_i as the following;

$$N_i = \left\{ C_j \mid dist\left(BS_i, BS_j\right) < d_{CS} \right\}$$

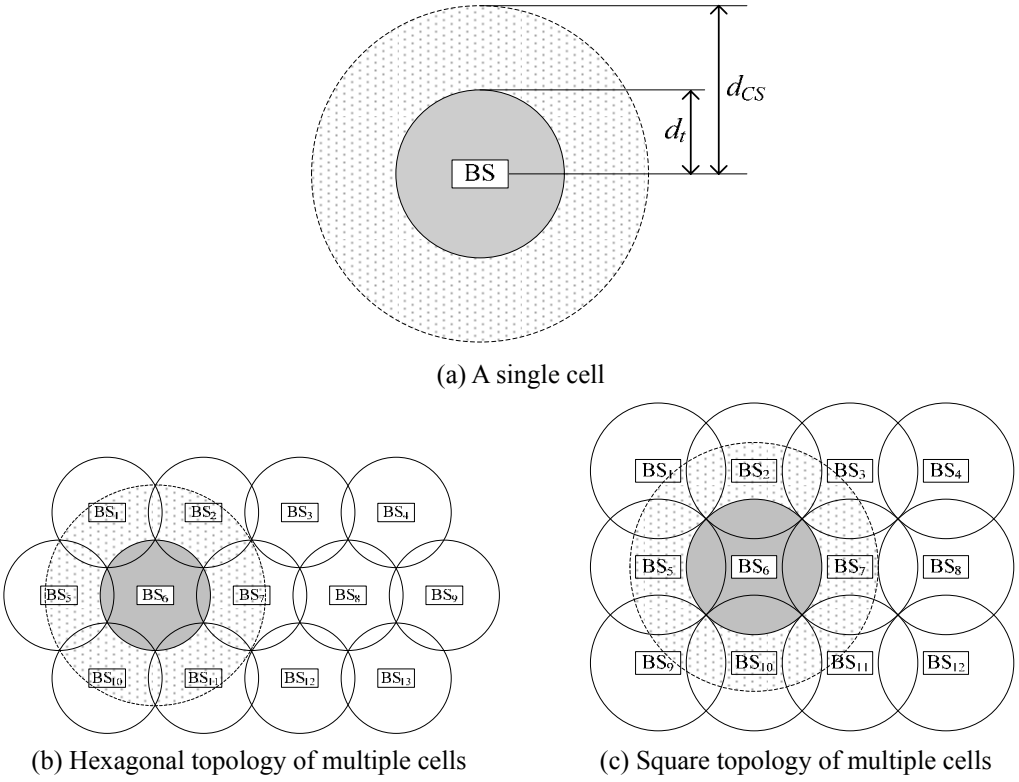

(a) A single cell

(b) Hexagonal topology of multiple cells

(c) Square topology of multiple cells

Figure 15. A cell in network topology and two examples of multi-cell networks

where $dist(BS_i,BS_j)$ is a distance between two base stations BS_i and BS_j. In Figure 15 (b), for example, N_6 is $\{C_1, C_2, C_5, C_7, C_{10}, C_{11}\}$. In the same way, N_6 in Figure 15 (c) is $\{C_2, C_5, C_7, C_{10}\}$.

In this work, we schedule cells so that a scheduled active cell C_i has no active neighbor cells. The input parameters are a set of all cells C, the number of cells m, unique cell IDs of all cells, and the sequence number of the current scheduling interval. The cell-level scheduling algorithm running on a cell C_i is shown in I.13. We assume that at the first run of this algorithm, one cell is specified as a starting point of scheduling. For example, $i = 1$. Beginning from this cell, we remove the scheduled cell C_i and its neighbor cells whenever a cell C_i is scheduled. We find the next cell C_j that is closest to C_i. However, C_j should

Cell-level scheduling algorithm ***- I.13***

1. Pick the first cell to schedule, C_i.
2. Add C_i to an assignment of scheduled active cells, $S \leftarrow S \cup \{C_i\}$.
3. Remove a scheduled cell C_i and its neighbor cells from C, $C \leftarrow C - (\{C_i\} \cup N_i)$
4. Find an unscheduled cell $C_j \in C$ which shares two neighbor cells with any scheduled cell, satisfying $C_j \in N_k$ and $C_j \in N_l$ for $C_k \in N_{i'}$, $C_l \in N_{i'}$, and $C_{i'} \in S$.
5. If $C_j \in C$ is found, update *i* to *j* and go to 2, $i \leftarrow j$
6. Otherwise, there is no more cell to schedule. Then, update *i* to *i+1*, and the algorithm terminates, $i \leftarrow i+1$

not be a neighbor cell of any scheduled cells. Step 4 of I.13 enforces this constraint. If C_j is not a neighbor cell of any scheduled cells, we schedule C_j. We repeat this process until we cannot find any more cells to schedule.

Examples of running this proposed cell-level scheduling algorithm are shown in Figure 16. We use two types of multi-cell topology; hexagonal and square multi-cells. In a hexagonal multi-cell network such as Figure 16 (a), the minimum number of time slots for scheduling all cells at least once is three. The active cells scheduled at the same time slot are indicated with the same letters (*A*, *B*, or *C*) and with the same color patterns. In the same way, we can schedule all cells in two time slots, *A* and *B*, in the case of square multi-cell topology shown in Figure 16 (b).

5. Combined running of cell-level and node-level scheduling

In the previous sections, we presented the centralized/distributed node-level

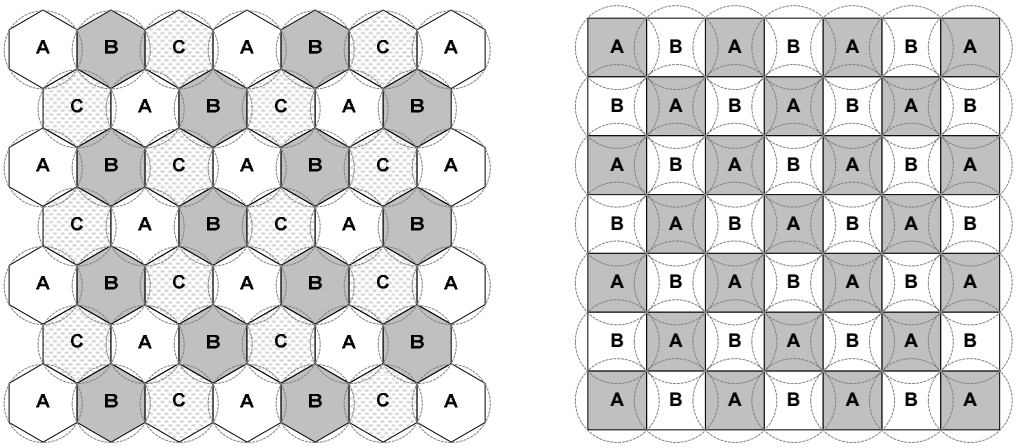

(a) Scheduled sets of cells in hexagonal topology (b) Scheduled sets of cells in square topology

Figure 16. Examples of cell-level scheduling

scheduling and the cell-level scheduling algorithms. We use both scheduling algorithms in scheduling wireless nodes in a multi-cell wireless network. In this section, we introduce how two scheduling algorithms run together.

Cell-level and node-level scheduling algorithms run at every scheduling interval. By running the cell-level scheduling algorithm, each base station decides if its cell is active in the next scheduling slot. The nodes also run the node-level scheduling algorithm. The node is active in the next scheduling slot only if it is scheduled by the result of node-level scheduling algorithm and if its cell is active. The schedule of a cell is announced to a new node when the node enters a network.

An example is shown in Figure 17. In this example, there are two cells C_1 and C_2, and eight nodes n_1, …, n_8. The nodes n_1, n_2, n_3, and n_4 are in Cell C_1, and the other nodes are in C_2. We use the same size of scheduling interval in cell-level scheduling and node-level scheduling. When C_1 is active, the nodes n_1 and n_2 run the node-level scheduling algorithm and find that they are scheduled in the coming scheduling slot.

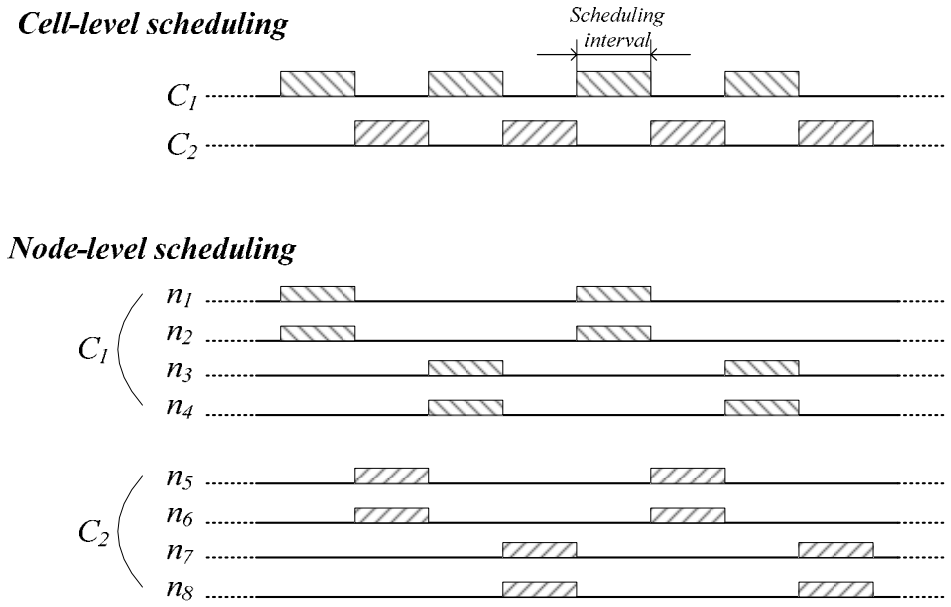

Figure 17. Combined running of cell-level and node-level scheduling

Subsequently, n_1 and n_2 wake up from a sleep mode and transmit their data to their base station. Since the other nodes n_3 and n_4 find that they are not scheduled, they wait for the next schedule in a sleep mode. Because C_2 is not active in the first scheduling slot, the nodes n_5, …, n_8 wait in the sleep mode even if the result of node-level scheduling algorithm says that they are schedulable.

In our combined scheduling, we use the same size of scheduling interval for both cell-level scheduling and node-level scheduling. It is also possible to use different slot sizes for two scheduling algorithms. For example, if we set the scheduling interval of cell-level scheduling as a double of node-level scheduling interval, we can schedule the nodes twice in active cells. In that case, the overhead is that the delay of application traffic in the nodes of inactive cells increases. Therefore, there is a tradeoff between more scheduling opportunities and longer delay.

Distributed cell- and node-level scheduler ***- I.14***

1. A new node n_i enters a cell C_j.
2. n_i registers itself to a cell-level scheduler at a base station of C_j and acquires the schedule of C_j from the cell-level scheduler.
3. n_i broadcasts its node ID to its neighbor nodes.
4. n_i gets the information on its two-hop topology from neighbor nodes.
5. n_i runs DNLS algorithm in I.12 at every scheduling interval. According to the determined schedule, proxy in n_i switches wireless interface and buffers/transmits data traffic from applications.

In this chapter, the scheduling problem we cover in this research has been introduced and defined. We describe an optimal scheduling algorithm and show that this optimal algorithm is NP-complete. We have presented the centralized node-level scheduling algorithm for a maximal scheduling. Next, we generalize it to make it work in a distributed manner. We illustrate how we can reduce the interference from neighbor cells by running a cell-level scheduling algorithm. Finally, we show how to combine the cell-level scheduling and the node-level scheduling algorithms for multi-cell networks. In the next chapter, we analyze the performance of our scheduling algorithms.

V. SIMULATION AND EVALUATION

In the previous chapter, we have presented our scheduling algorithm, which consists of cell-level scheduling and node-level scheduling. In this chapter, we first describe the design of a proxy layer in which our scheduling algorithm is implemented. The simulation setup and parameters are shown in the next section. Then, we examine the performance of the proposed scheduling algorithm by running simulations on *ns*-2 network simulator. We present the results for two types of data traffic; 1) high traffic constant-bit-rate (CBR) data and 2) real data traffic. Our evaluation with real traffic traces shows power saving of 85.54% and throughput gains of up to 10.31%.

1. Proxy layer design

In order to provide an easily adaptable design, we implement our scheduling algorithm in two parts; a proxy and a scheduler, as can be seen in Figure 18. The proxy layer, or *proxy* for short, is a protocol layer between network/transport layers in the kernel and the application layer of actual applications running on wireless nodes. The proxy uses the network socket interface provided by the transport layer, and it also gives seamless interface to applications. Once application data traffic is delivered to a proxy, the data is passed through the network if the node is in an active mode. Otherwise, data is buffered in a proxy while the node is asleep. Buffered data is delivered after the node is scheduled to be active.

The *scheduler* is an application process that determines when a node can access the radio channel. Our proposed scheduling algorithm resides in the scheduler. The scheduler is tightly integrated with a proxy. We have two types of schedulers. The cell level scheduler running on base stations determines when the corresponding cell is scheduled. The schedule of a node is decided by the node-level scheduler running over a proxy layer of nodes. The

schedule decided by the node-level scheduler is passed to a proxy, which controls the power mode of a wireless device according to the schedule.

2. Simulation setup

To evaluate performance and overhead of the proposed scheduling algorithm, we run simulations on *ns-2* network simulator [3]. The detailed simulation parameters used in our

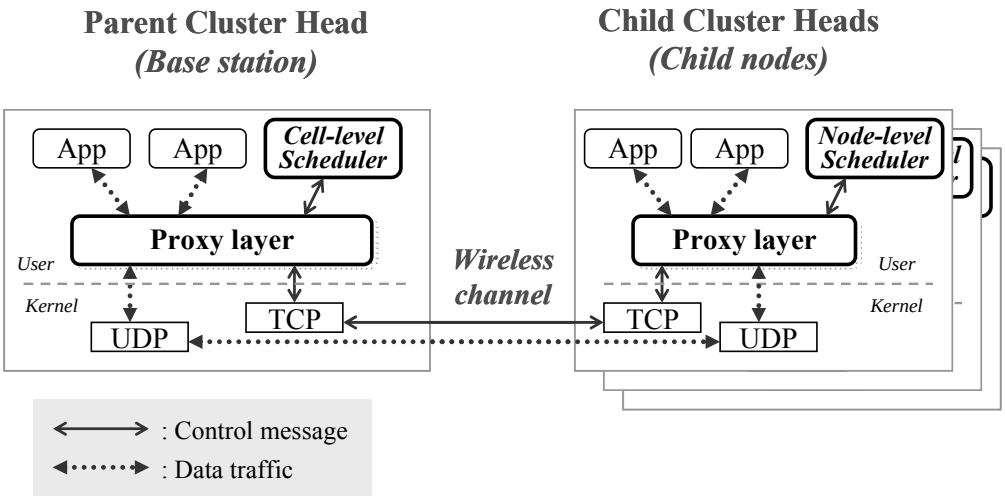

Figure 18. Implementation of scheduler and proxy

simulations are shown in Table 1. Simulation parameters for 802.11b are appropriate for the typical IEEE 802.11b wireless channels [39] [40]. The parameters for power in each power mode are from the data sheet of the *Cisco Aironet* wireless LAN adapter [1]. The transition time for power modes is from the measurement results presented in [16].

Simulations are performed on two types of network topologies; hexagonal cells and square cells. The topology and the deployment of cells used in our simulations are shown in Figure 19. The sizes of network topologies are 533m by 550m for hexagonal multi-cell networks, and 524m by 524m for square multi-cell networks respectively. The hexagonal topology has 39 cells, and the square topology 49 cells. The radius of each cell is equal to d_t =

50m. The base stations are at the center of each cell, and every child node in the cell can communicate with a base station. Cells are located such that any space is covered by at least one cell, except for the boundary area.

On the given network topology, we test two types of data traffic. The first one is CBR

Table 1. Simulation parameters in *ns2*

PARAMETER	MEANING	VALUE
d_t	Communication range	50 m
d_{CS}	Carrier-sensing range	99 m
P_{idle}	Power of WNIC in idle mode	0.6698 W
P_{TX}	Power of WNIC in transmitting a packet	1.0791 W
P_{RX}	Power of WNIC in receiving a packet	1.7789 W
P_{sleep}	Power of WNIC in sleep mode	0.0495 W
$P_{idle\_to\_sleep}$	Transition power from an idle mode to a sleep mode	0.6698 W
$P_{sleep\_to\_idle}$	Transition power from a sleep mode to an idle mode	0.6698 W
$T_{idle\_to\_sleep}$	Transition time from an idle mode to a sleep mode	0.4 ms
$T_{sleep\_to\_idle}$	Transition time from a sleep mode to an idle mode	20 ms
P_t	Transmitted signal power	0.031622777
CP_{Thresh}	Collision threshold	10.0
CS_{Thresh}	Carrier sense power	3.00923e-10
RX_{Thresh}	Receive power threshold	1.17974e-09

MEANING	VALUE
Propagation model	Propagation/TwoRayGround
Antenna model	Antenna/OmniAntenna
RTS threshold	4095 bytes
Channel frequency	2.472 GHz (channel 13)
Data traffic type	UDP
Packet size of data traffic	1000 bytes
Basic rate of channel	1 Mbps
Data rate of channel	11 Mbps

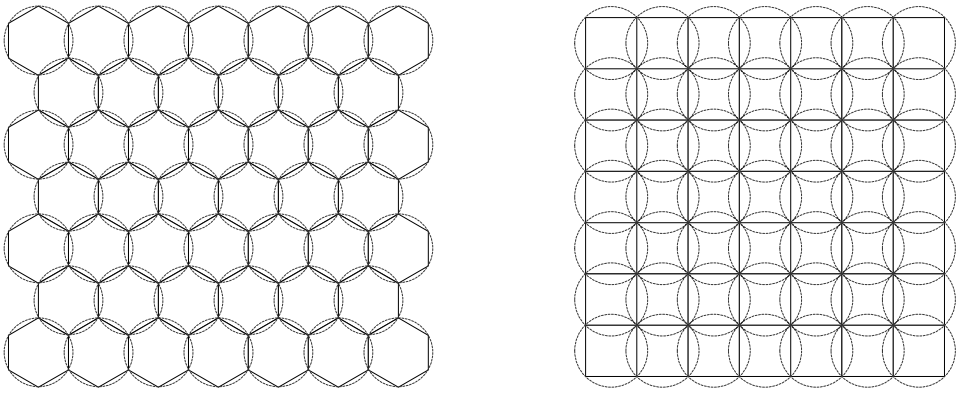

(a) Hexagonal multi-cell topology (b) Square multi-cell topology

Figure 19. Multi-cell topology used in simulations

traffic with a very high data rate. This traffic tests the situation where the MAC layer input queues are always full of data packets. Therefore, traffic load is always above the saturation throughput of the network. We call this *CBR traffic in full MAC queues*. We vary the number of child nodes in a cell, which is defined as the *node density*. The node density is the average number of child nodes in the circular area with a radius of d_t. Since the size of a cell in our topology is a little smaller than the size of a circular cell, the actual number of child nodes per cell in our networks is not equal to the given node density. The range of node density used in our simulations is 2 to 20.

The second type of data traffic is real data traffic. We use a data traffic trace collected from a cluster head in the SMER network of the HPWERN. Other cluster heads show the same traffic pattern. From this traffic trace, we synthesize the data traffic for up to 675 other cluster heads in the maximum node density. These data traffic traces are used in simulating the case where a large number of child cluster heads transmit data traffic to parent cluster heads in a multi-cell wireless network. The average data rate of the traffic trace from a single child cluster head is 136 Kbps.

Another important factor in our scheduling algorithm is s; the number of contending

nodes within a communication range. This number is dependent on the configuration and the environment of a given network. By measuring the aggregate throughput in a real wireless network, we can choose the parameter value suitable for a given network. In general, however, our simulation result for 802.11b in Section III.2 shows that the maximum throughput is achieved when 2 ~ 4 contending nodes access the channel. Considering the nodes with less traffic load, we use $s = 4$ for the simulations in multi-cell wireless networks.

In the following sections, we present the simulation results with two types of data traffic; CBR traffic in full MAC queues and real data traffic. In each case, we show that our scheduling give a significant saving in communication power as well as an improvement in the throughput. In the last section, we consider the tradeoff between different scheduling slot sizes.

3. Results for the CBR traffic in full MAC queues

We first measure the performance of scheduling against the CBR traffic model with a high data rate. In this model, each child node generates very high rate of data traffic so that MAC layer queues are always full. Therefore, we can see the performance in the case where traffic load is very heavy. In this section, we show three types of simulation results; 1) the case without scheduling, 2) with centralized node-level scheduling (CNLS), and 3) with distributed node-level scheduling (DNLS). The cases for both CNLS and DNLS use the same cell-level scheduling algorithm. The size of scheduling interval is shown in a legend of each figure.

The first important advantage of our scheduling is saving in communication power. The simulation results for average communication power per node are shown in Figure 20 (a) and Figure 20 (b). In both network topologies, an enormous amount of power is saved by running scheduling. This power saving is acquired by switching inactive nodes into a sleep mode. In Figure 20, the power saving in (b) square multi-cell is less than in (a) hexagonal

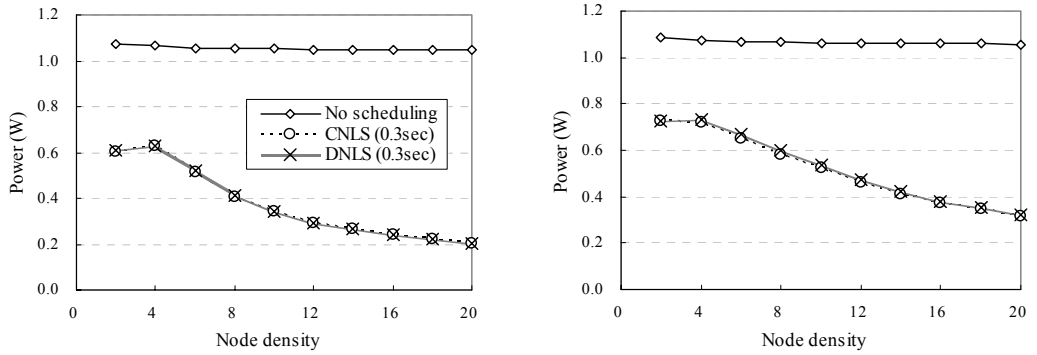

(a) Power in hexagonal multi-cell

(b) Power in square multi-cell

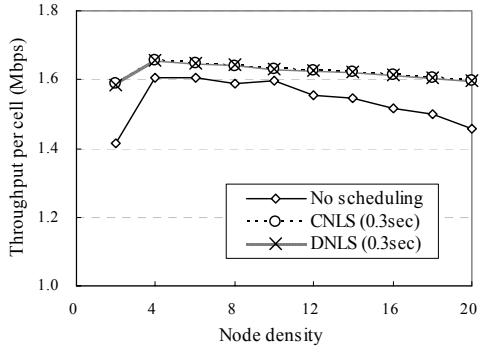

(c) Throughput in hexagonal multi-cell

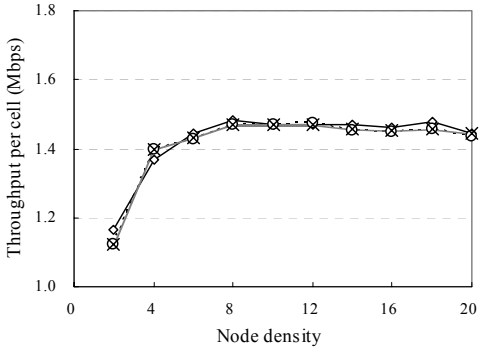

(d) Throughput in square multi-cell

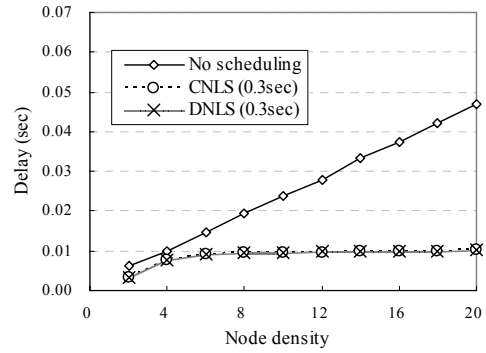

(e) Transmission delay in hexagonal multi-cell

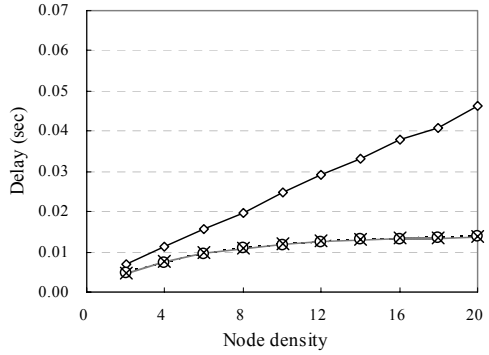

(f) Transmission delay in square multi-cell

Figure 20.Results for the CBR traffic model

multi-cell. This is because cells in square multi-cell topology are scheduled more often, every two time slots. As the node density increases, we get higher power saving. When the node density is high, a node has a lower chance of being scheduled. Accordingly, we get more power savings. Maximum power savings reach up to 80%.

The next point to consider is throughput. The throughput is measured at the base

stations. Figure 20 (c) and (d) show the measured average throughput for the CBR traffic in full MAC queues. In Figure 20 (c), we find that scheduling improves the average throughput significantly. This improvement is due to the reduction of contention in the radio channel. To understand how much time is spent in transmitting a packet on the MAC layer, we measured the transmission delay of a data packet. Transmission delay is defined as the delay from the receipt of a data packet at MAC layer until a data packet is acknowledged by an ACK packet in the MAC layer, coming from a receiver node. The measured result is shown in Figure 20 (e) and (f). In both topologies, transmission delay increases gradually as the network density goes up. By running our scheduling algorithm, we can control the transmission delay at the same level as the delay for a network with the node density of 4. Thus, we can say that the amount of contention by running our scheduling is very close to the case when only four nodes contend for accessing the channel within a communication range.

We also find that two scheduling algorithms, centralized node-level scheduling (CNLS) algorithm and distributed node-level scheduling (DNLS) algorithm, give very similar results in communication power and throughput. This is because two algorithms schedule almost the same number of child nodes in an active cell. This means that the performance of DNLS algorithm is very close to that of CNLS algorithm. In terms of the number of scheduled active nodes, DNLS algorithm gives the result very close to that of CNLS algorithm. If the number of active nodes is too small, we get lower average throughput because the active nodes cannot fully exploit available channel bandwidth. If the number of nodes scheduled by DNLS algorithm is too large, we cannot reduce the contention in a channel enough. Thus, we get the lower throughput. In the other performance metrics such as power and delay, we observe the same results. Therefore, from the next section, we only present the results for the DNLS algorithm.

The difference in simulation results between hexagonal and square multi-cell topologies is substantial. From the result in Figure 20 (d), we see that average throughput is not improved by our scheduling. As explained in the algorithm description of Chapter IV, the current cell-level scheduling algorithm in square multi-cell topology schedules a cell every two scheduling time slots. Though this strategy decrease a lot of interference from neighboring cells, active cells still experience interference from the other active cells. In the square multi-cell topology, the distance between the centers of two active cells is equal to carrier-sensing range. Thus, the active nodes still suffer from interference from other active nodes in surrounding active cells. Figure 21 (a) shows this scheduling strategy. Cells marked with the same letters are scheduled in the same time slot.

One solution for excessive interference between active cells is to increase the distance between scheduled active cells. For example, it is possible to schedule a cell every four scheduling time slots, rather than every two scheduling time slots. Figure 21 (b) represents the strategy of scheduling cells every four time slots. With this strategy, the distance between

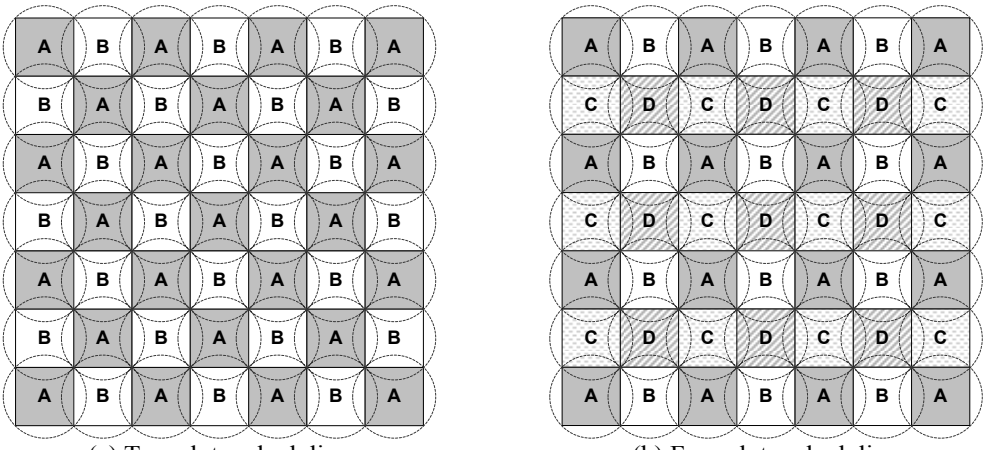

(a) Two-slots scheduling (b) Four-slots scheduling

Figure 21. Two strategies for cell-level scheduling in square multi-cell

active cells is far enough to completely remove interference among active cells. But, this scheme reveals a critical disadvantage in improving throughput. Because the number of active cells for a time slot is smaller in four-slots scheduling of Figure 21 (b) than in two-slots scheduling of Figure 21 (a), it is very difficult for a four-slot scheduling to achieve any improvement in throughput. Therefore, the average throughput by four-slots scheduling of Figure 21 (b) is less than in the case without any scheduling at all. In other words, we can say that active cell's spatial parallelism in a network topology is an important factor in determining the throughput improvement achievable by scheduling. In a hexagonal multi-cell topology, locations of active cells maximize scheduling throughput gain because the active cells are far enough to eliminate most of interference between active cells while they are close enough to exploit spatial parallelism in a given field area. Therefore, by running the scheduling over an appropriate network topology, we can get more benefits than just reduced power, e.g., throughput gain.

4. Results for the real data traffic

We next take a look at the simulation results from real data traffic. The CBR traffic model in the previous section is to measure the performance under the heavy traffic loads. In this section, the simulation with real data traffic shows how our scheduling performs in the case where a network contains a large number of the child cluster heads. The results on communication power, average throughput per cell, and MAC layer transmission delay are presented. In addition, we discuss the application layer delay in detail.

We first observe great power savings when running scheduling in both hexagonal and square multi-cell topology. In Figure 22 (a) and (b), DNLS-based scheduling saves up to 85.54 % of communication power in the hexagonal multi-cell case and up to 78.63 % in the square multi-cell case. The higher power savings in hexagonal case are due to the longer sleep

period from the cell-level scheduling. The observed values of communication power for the case with no scheduling show a different pattern from the values in Figure 20. In Figure 20 (a) and (b), we see that communication power is almost flat. However, in Figure 22 (a) and (b), the power increases gradually until it becomes saturated. At the full MAC-layer queue model in Figure 20, the network channel is always congested by traffic since MAC layer queues in nodes are always full. But the nodes of the real traffic model in Figure 22 have an average data rate of 136 Kbps. Until the network channel is fully congested by traffic, wireless devices work in an idle mode for the large amount of time. While it is in an idle mode, wireless devices consume less power. Therefore, the communication power in the real-traffic model is less than the power in high data rate CBR model until the network channel is saturated by data traffic. In both of Figure 20 and Figure 22, our scheduling achieves significant power savings.

Average throughput and MAC layer transmission delay are shown from Figure 22 (c) to (f). In a hexagonal multi-cell topology, we see that our scheduling improves the average throughput when traffic load is above the saturation level of the network, which is 1.1 Mbps without scheduling. The throughput gained by scheduling is up to 10.31 %. In the square multi-cell topology, however, we find a different result. In this case, running our scheduling only decreases the throughput up to 7.27 %. As pointed out in the previous section and in Figure 20, this is caused by the distribution of active cells in square multi-cell topology that is too dense to eliminate interference from other active cells. In a square multi-cell, the distance between active cells is not far enough to remove most of inter-cell interference. Therefore each active cell cannot obtain the maximum throughput.

We next discuss the application layer delay. Application layer delay is the time delay that applications running on wireless nodes experience. This is the actual delay in delivering a fixed-size data packet from a sender application to a receiver application. Using our

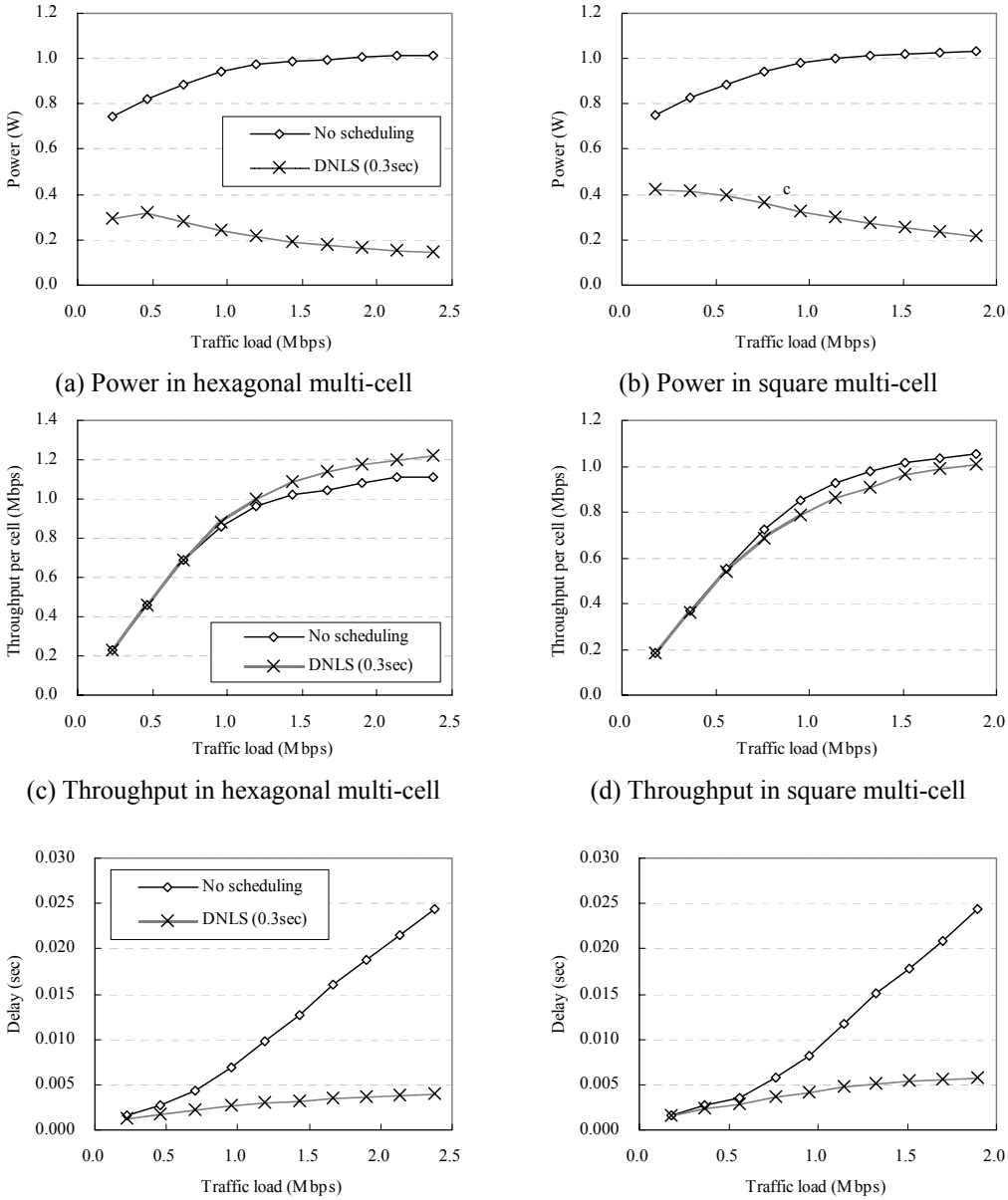

(a) Power in hexagonal multi-cell

(b) Power in square multi-cell

(c) Throughput in hexagonal multi-cell

(d) Throughput in square multi-cell

(e) Transmission delay in hexagonal multi-cell

(f) Transmission delay in square multi-cell

Figure 22. Results for the real traffic data model

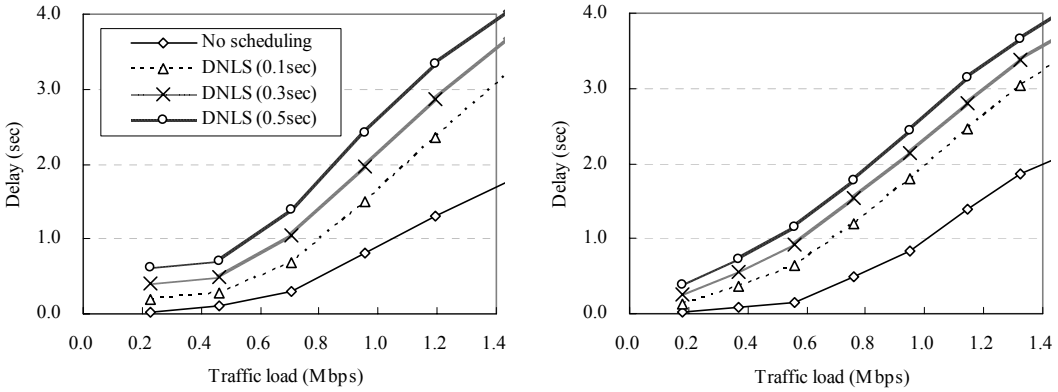

(a) Delay in hexagonal multi-cell (b) Delay in square multi-cell

Figure 23. Application layer delay in a real-traffic model

scheduling algorithm on a given network reduces the number of contending nodes in a channel. Consequently, the MAC layer delay is reduced. However, because of the scheduling interval based scheme of our scheduling algorithm, it is inevitable that the actual application layer delay increases accordingly. The results on application layer delay for the real-traffic model are shown in Figure 23. We limit the maximum value of the horizontal axis, the amount of traffic load, to 1.4 Mbps. Once the traffic load exceeds the maximum throughput experienced by the case with no scheduling (which is 1.1 Mbps in Figure 22 (a) and (b)), application layer delay increases dramatically.

For the cases of Figure 23 where scheduling is applied, applications experience a certain level of application layer delay; in the case of the scheduling slot size of 0.3 second, delay is at least 0.4 second in the hexagonal and 0.26 seconds in the square multi-cell. This delay is due to the unscheduled nodes that wait in a sleep mode while buffering data from applications. We also see a difference in the minimum amount of delay between the two topologies. The square multi-cell topology experiences a lower value in the minimum delay. This is because the cell-level scheduling algorithm uses two time slots for scheduling all cells,

while it schedules a cell in the hexagonal multi-cell every three time slots. Therefore, the nodes in the square multi-cell topology get more of a chance to send their traffic than nodes in the hexagonal multi-cell. This results in a shorter delay for the square multi-cell.

It is unavoidable to experience a certain level of application layer delay in scheduling techniques which use a sleep mode of interface device. However, it is possible to reduce that delay by prioritizing traffic, such as with weighted fair queueing [10]. Another way to reduce the application layer delay is by minimizing the size of the scheduling slots. Thus we next study the effects of different slot sizes. With the previous full MAC-queue model simulations in Section V.3, we used the slot size of 0.3 seconds. To know how different slot sizes affect the performance of scheduling, we run the same simulations with three slot sizes; 0.1 seconds, 0.2 seconds, and 0.3 seconds.

The results on the average throughput and communication power with different slot sizes are shown in Figure 24. In Figure 24 (a) and (b), we see that the amount of overhead in scheduling is inversely proportional to the length of the scheduling slot. If the scheduling slot is short, nodes switch their modes more frequently. This phenomenon causes more mode transitions. Between scheduling intervals, more than s active nodes contend for accessing the channel for a short period of time. Since the advantage of scheduling in terms of throughput is achieved by limiting the number of active nodes to a given factor s, we cannot get much of a throughput improvement around the mode transitions. Therefore, frequent mode transitions result in the reduction of throughput. In both Figure 24 (a) and (b), the cases with the shorter scheduling slot sizes experience a lower average throughput.

The overhead from shorter scheduling sizes is also found in the simulation results for communication power. While the wireless interface switches its mode, it consumes at least as much power as it does in an idle mode. Mode transition also takes a certain transition time to

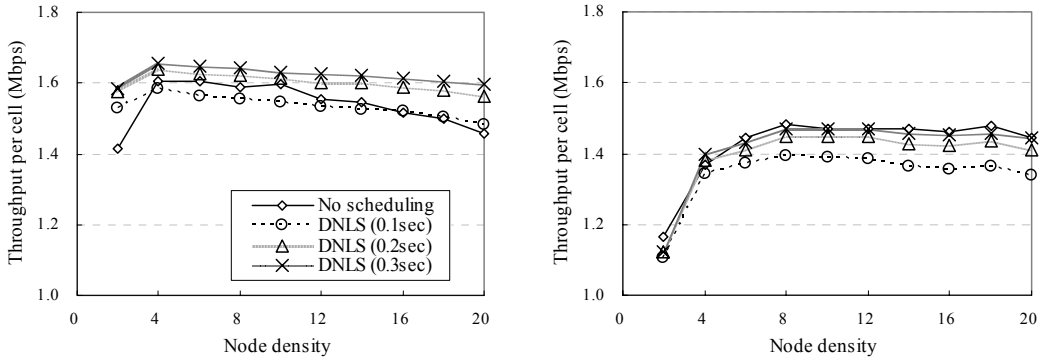

(a) Throughput in hexagonal multi-cell (b) Throughput in square multi-cell

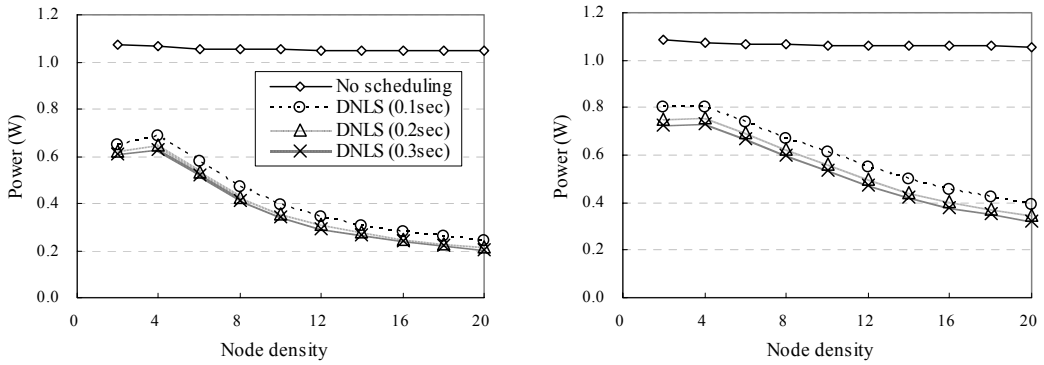

(c) Power in hexagonal multi-cell (d) Power in square multi-cell

Figure 24. Throughput and power for different slot sizes

wake up and to go sleep. Specific parameters are in Table 1 in the previous chapter. Thus, it is expected that scheduling with the shorter slot size reveals more overhead in energy consumption. The results in Figure 24 (c) and (d) show that the overhead in power increases as the slot size decreases.

From the perspective of throughput and power, we can say that it is better to use a longer stretch for the scheduling time slot. The use of a longer scheduling slot improves the average throughput and saves more communication power, but causes a longer delay. The tradeoff between the improvements in throughput and power and the cost in terms of delay is a key issue in determining the scheduling slot size.

In this chapter, we have evaluated our scheduling algorithms by running simulations with two types of data traffic patterns. We achieve large amount of communication power savings: up to 80.38% for CBR traffic and up to 85.45% for real data traffic. The maximum throughput gains are 9.48% and 10.24% respectively.

VI. CONCLUSIONS

In this thesis, we have presented a hybrid distributed multi-cell scheduling algorithm. We have shown that a falloff in an aggregate throughput in a large-scale multi-cell wireless network is due to both interference between neighboring cells and the contention among nodes. To remove interference between cells, we presented a distributed cell-level scheduling algorithm. To solve the problem of contention among nodes, we proposed an optimal node-level scheduling algorithm for a maximum scheduling. Moreover, we proved that the algorithm for a maximum scheduling is NP-complete for any $s \geq 1$. Because running an NP-complete algorithm at runtime is not practical in large-scale multi-cell wireless networks, we proposed the centralized node-level scheduling algorithm that is a solution for the simpler maximal scheduling problem. Next, we converted this algorithm into a distributed node-level scheduling algorithm. Finally, we combined the cell-level scheduling and the node-level scheduling algorithms to run our scheduling in a wireless network consisting of large number of cells.

Our proposed scheduling algorithms run on a proxy layer. Proxy is a virtualization mechanism that provides a seamless application interface while minimizing modification of existing network protocol implementation in the kernel. By running the scheduling algorithms on the proxy layer, we are able to show that a novel scheduling algorithm can run over the existing network and MAC layers, using off-the-shelf network components.

The proposed scheduling algorithm runs on multi-cell heterogeneous wireless networks. Our scheduling mechanism provides the control of channel access and throughput allocation to the sensor node cluster heads. We can get an improvement in aggregate throughput by reducing both the contention between the nodes and the interference between

the neighboring cells. Saving communication power while achieving an increase in throughput is a big accomplishment of our proposed algorithm.

To evaluate the performance of the proposed scheduling algorithm in a real network, we have run the simulations with the real traces of data traffic collected at the cluster head nodes in the SMER network. In those experiments, we see an improvement in average throughput of up to 10.31 % in hexagonal multi-cell networks, with maximum power saving of 85.54 %.

We also measured the overhead of scheduling on delay in data delivery. By measuring the application layer delay of delivered data traffic, we concluded that the size of scheduling time slot determines the minimum possible delay. Different scheduling slot sizes affect the overhead in throughput, power saving, and delay. Therefore, it is important to find the right tradeoff between the benefits of scheduling and the cost in delay. With the current randomized scheduling algorithm we recommend choosing a longer scheduling slot size if the delay requirements of applications are satisfied. In addition, the application layer delay can be further optimized by introducing traffic priorities. We leave this for future work.

VII. REFERENCES

[1] Cisco Aironet 802.11a/b/g CardBus wireless LAN adapter data sheet, http://www.cisco.com/en/US/products/hw/wireless/ps4555/products_data_sheet09186a00801ebc29.html, Cisco Systems.

[2] High Performance Wireless Research and Education Network (HPWREN), *http://hpwren.ucsd.edu/*

[3] ns-2 network simulator, *http://www.isi.edu/nsnam/ns/*

[4] G. Ahn, A. T. Campbell, A. Veres, and L. Sun, "SWAN: Service differentiation in stateless wireless ad hoc networks," in *IEEE INFOCOM*, 2002.

[5] E. Arikan, "Multi-access in packet-radio networks," M.Sc. thesis, MIT, LIDS-TH-1234, 1982.

[6] M. Bottigliengo, C. Casetti, C. Chiasserini, and M. Meo, "Smart traffic scheduling in 802.11 WLANs with access point," *IEEE Vehicular Technology Conference,* 2003.

[7] R. Bruno, M. Conti, and E. Gregori, "Mesh networks: commodity multihop ad hoc networks," *IEEE Communications Magazine*, 2005.

[8] S. Choi, K. Park, and C. Kim, "On the performance characteristics of WLANs: revisited," *ACM SIGMETRICS*, 2005.

[9] I. Cidon, and M. Sidi, "Distributed assignment algorithms for multihop packet radio networks," *IEEE Transactions on Computers*, 1989.

[10] A. Demers, "Analysis and simulation of a fair queueing algorithm," *ACM SIGCOMM*, 1989.

[11] T. Elbatt and A. Ephremides, "Joint scheduling and power control for wireless ad hoc networks," *IEEE Transactions on Wireless Communications*, 2004.

[12] V. Gambiroza, B. Sadeghi, and E. W. Knightly, "End-to-end performance and fairness in multihop wireless backhaul networks," *MOBICOM*, 2004.

[13] W. K. Hale, "Frequency assignment: theory and applications," *Proc. IEEE*, 1980.

[14] M. Heusse, F. Rousseau, G. Berger-Sabbatel, and A. Duda, "Performance anomaly of 802.11b," *IEEE INFOCOM*, 2003.

[15] B. Hohlt, L. Doherty, and E. Brewer, "Flexible power scheduling for sensor networks," *International Symposium on Information Processing in Sensor Networks (IPSN)*, 2004.

[16] K. Jamieson, "Implementation of a power-saving protocol for ad hoc wireless networks", Master's thesis, *Massachusetts Institute of Technology*, Feb. 2002.

[17] J. Jun, P. Peddabachagari, M. Sichitiu, "Theoretical maximum throughput of IEEE 802.11 and its applications," *IEEE International Symposium on Network Computing and Applications*, 2003.

[18] E. Jung and N. H. Vaidya, "An energy efficient MAC protocol for wireless LANs," in *IEEE INFOCOM*, 2002.

[19] R. Karrer, A. Sabharwal, and E. Knightly, "Enabling large-scale wireless broadband: the case for TAPs," *ACM SIGCOMM Computer Communications Review*, 2004.

[20] L. Kleinrock and F. Tobagi, "Packet Switching in Radio Channels Part II - the Hidden Node Problem in Carrier Sense Multiple Access Nodes and the Busy Tone Solution," in *IEEE Transactions on Communications*, vol. COM-23, no. 12, pp. 1417-1433, 1975.

[21] D. Lim, J. Shim, T. S. Rosing, and T. Javidi, "Scheduling data delivery in heterogeneous wireless sensor networks," in *IEEE International Symposium on Multimedia (ISM 2006)*, Dec. 2006.

[22] S. Mangold, S. Choi, P. May, O. Klein, G. Hiertz, and L. Stibor, "IEEE 802.11e wireless LAN for quality of service," *European Wireless*, 2002.

[23] V. Mhatre and C. Rosenberg, "Homogeneous vs heterogeneous clustered sensor networks: a comparative study," *IEEE International Conference on Communications*, 2004.

[24] M. Petrovic and M. Aboelaze, "Performance of TCP/UDP under ad hoc IEEE 802.11," *International Conference on Telecommunications,* 2003.

[25] L. Pond and V. Li, "A distributed time-slot assignment protocol for mobile multi-hop broadcast packet radio networks," *IEEE MILCOM*, 1989.

[26] W. Qadeer, T. Simunic, J. Ankcorn, V. Krishnan, and G. D. Micheli, "Heterogeneous wireless network management," *Power-Aware Computer Systems*, 2003.

[27] R. Ramaswami, and K. Parhi, "Distributed scheduling of broadcasts in a radio network," IEEE INFOCOM, 1989.

[28] A. Rao and I. Stoica, "An overlay MAC layer for 802.11 networks," *ACM MOBICOM*, 2005.

[29] P. A. Raymond, "Performance analysis of cellular networks," *IEEE Transactions of Communications*, 1991.

[30] J. Rexford, S. Sen, and A. Basso, "A smoothing proxy service for variable-bit-rate streaming video," in *IEEE GLOBECOM*, 1999.

[31] B. Sadeghi, V. Kanodia, A. Sabharwal, and E. Knightly, "Opportunistic media access for multirate ad hoc networks," *ACM MOBICOM*, September, 2002, Atlanta, Georgia.

[32] P. Shenoy and P. Radkov, "Proxy-assisted power-friendly streaming to mobile devices," *Multimedia Computing and Networking,* 2003.

[33] T. Simunic, W. Qadeer, and G. D. Micheli, "Managing heterogeneous wireless environments via Hotspot servers," *Multimedia Computing and Networking*, 2005.

[34] J. Snow, W. Feng, and W. Feng, "Implementing a low power TDMA protocol over 802.11," *IEEE Wireless Communications and Networking Conference*, 2005.

[35] N. H. Vaidya, P. Bahl, and S. Gupta, "Distributed fair scheduling in a wireless LAN", *ACM MOBICOM*, 2000.

[36] A. Vasan and A.U. Shankar, "An empirical characterization of instantaneous throughput in 802.11b WLANs," Technical report, *Department of Computer Science, University of Maryland*, 2002.

[37] S. Waharte, J. Xiao, and R. Boutaba, "Overlay wireless sensor networks for application-adaptive scheduling in WLAN," *IEEE Conference on High Speed Networks and Multimedia Communications,* 2004.

[38] H. Wu, Q. Luo, and W. Xue, "Distributed cross-layer scheduling for in-network sensor query processing," *IEEE International Conference on Pervasive Computing and Communications (PERCOM)*, 2006.

[39] W. Xiuchao, "Simulate 802.11b channel within ns2", Technical report, School of Computing, National University of Singapore , 2004.

[40] W. Xiuchao and A. L. Ananda, "Link characteristics estimation for IEEE 802.11 DCF based LAN," *IEEE Conference on Local Computer Networks*, 2004.

[41] Y. Yi and S. Shakkottai, "Hop-by-hop congestion control over a wireless multi-hop network," *IEEE INFOCOM*, 2004.

[42] F. Yu, Q. Zhang, W. Zhu, and Y. Zhang, "QoS-adaptive proxy caching for multimedia streaming over the internet," in *IEEE Transactions on Circuits and Systems for Video Technology*, Vol. 13, No. 3, March 2003.

[43] J. Zander, "Performance of optimum transmitter power control in cellular radio systems," *IEEE Transactions on Vehicular Technology*, 1992

[44] H. Zhai, J. Wang, and Y. Fang, "Distributed packet scheduling for multihop flows in ad hoc networks," *IEEE Wireless Communications and Networking Conference*, 2004.